AD-A086 653 NORTHWESTERN UNIV EVANSTON IL DEPT OF MATERIALS SCIENCE F/G 11/2
FRACTURE STUDIES OF HIGH TEMPERATURE CERAMICS.(U)
MAY 80 D L JOHNSON AFOSR-76-2920

UNCLASSIFIED AFOSR-TR-80-0501 NL

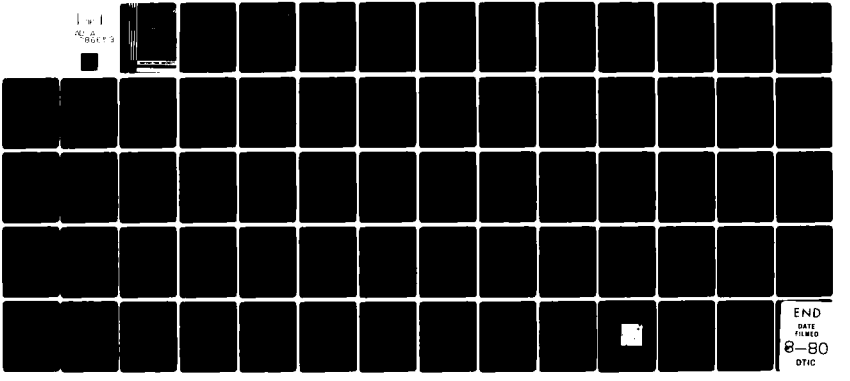

END
DATE FILMED
8-80
DTIC

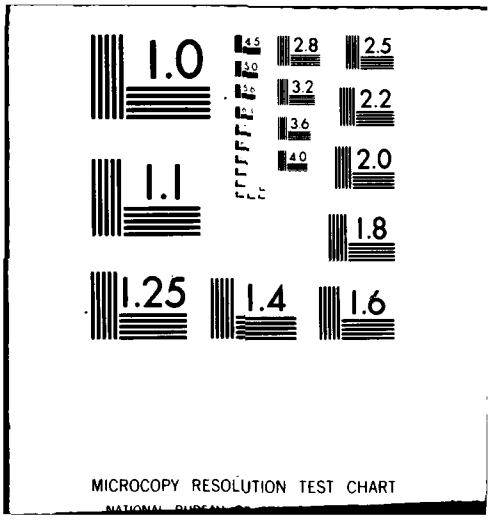
1.0
1.1
1.25
1.4
1.6
1.8
2.0
2.2
2.5
2.8
3.2
3.6
4.0
4.5
5.0
MICROCOPY RESOLUTION TEST CHART

AFOSR-TR- 80-0501

LEVEL II

Approved for public release;
distribution unlimited.

FINAL REPORT

on

FRACTURE STUDIES OF HIGH TEMPERATURE CERAMICS

Covering Period

1 October 1975 to 30 September 1979

by

D. Lynn Johnson

May 1980

This research was supported by AFOSR under Grant No. AFOSR-76-2920[redacted]

Department of Materials Science and Engineering
Northwestern University
Evanston, Illinois 60201

Approved for public release; distribution unlimited

AIR FORCE OFFICE OF SCIENTIFIC RESEARCH (AFSC)
NOTICE OF TRANSMITTAL TO DDC
This technical report has been reviewed and is approved for public release IAW AFR 190-12 (7b).
Distribution is unlimited.
A. D. BLOSE
Technical Information Officer

80 7 2 041

Unclassified

SECURITY CLASSIFICATION OF THIS PAGE (When Data Entered)

REPORT DOCUMENTATION PAGE	READ INSTRUCTIONS BEFORE COMPLETING FORM
1. REPORT NUMBER (19) (18) AFOSR-TR-80-0501	2. GOVT ACCESSION NO. AD-A086653	3. RECIPIENT'S CATALOG NUMBER
4. TITLE (and Subtitle) (6) FRACTURE STUDIES OF HIGH TEMPERATURE CERAMICS,	5. TYPE OF REPORT & PERIOD COVERED (9) Final rept. 1 Oct 75 — 30 Sep 79,
	6. PERFORMING ORG. REPORT NUMBER
7. AUTHOR(s) (10) D. Lynn Johnson	8. CONTRACT OR GRANT NUMBER(s) AFOSR-76-2920
9. PERFORMING ORGANIZATION NAME AND ADDRESS Department of Materials Science and Engineering Northwestern University Evanston, Illinois 60201	10. PROGRAM ELEMENT, PROJECT, TASK AREA & WORK UNIT NUMBERS 61102F, 2306/A2
11. CONTROLLING OFFICE NAME AND ADDRESS Air Force Office of Scientific Research/NE Bldg. 410 Bolling AFB, D.C. 20332	12. REPORT DATE May 1980 (12) 67
	13. NUMBER OF PAGES 65
14. MONITORING AGENCY NAME & ADDRESS(if different from Controlling Office) (16) 2306 (17) A2	15. SECURITY CLASS. (of this report) Unclassified
	15a. DECLASSIFICATION/DOWNGRADING SCHEDULE

16. DISTRIBUTION STATEMENT (of this Report)

Approved for public release; distribution unlimited.

17. DISTRIBUTION STATEMENT (of the abstract entered in Block 20, if different from Report)

(15) AFOSR-76-2920, NSF-DMR 76-80847

18. SUPPLEMENTARY NOTES

(11) May 80

19. KEY WORDS (Continue on reverse side if necessary and identify by block number)

Ceramics, high temperature impact, high temperature fracture, silicon carbide, silicon nitride.

20. ABSTRACT (Continue on reverse side if necessary and identify by block number)

A high-temperature isothermal instrumented impact testing apparatus was designed and built and utilized to test a variety of high performance ceramic materials at temperatures up to 1500°C. Test specimens were held on an anvil in the furnace and heated rapidly to the test temperature. An impacter broke the samples in 3-point bending, and high speed digital recorders stored the outputs of force and velocity transducers. The controlled flaw technique was utilized to obtain the critical stress intensity factor, K_{IC}. Hot-pressed

DD FORM 1 JAN 73 1473 EDITION OF 1 NOV 65 IS OBSOLETE

Unclassified 260820

SECURITY CLASSIFICATION OF THIS PAGE (When Data Entered)

20. Abstract, continued.

silicon nitride materials containing MgO, CeO_2 or ZrO_2 sintering aids showed a decrease in K_{IC} as the temperature exceeded 1300°C. Hot-pressed silicon carbide containing alumina sintering aid showed a similar decrease. Sintered α-SiC, on the other hand, showed a gradual increase in K_{IC} at temperatures up to 1500°C. Reaction bonded SiC failed to break at the controlled flaw, but exhibited a drop in impact fracture force at temperatures approaching the melting point of silicon.

ABSTRACT

A high temperature isothermal instrumented impact resting apparatus was designed and built and utilized to test a variety of high performance ceramic materials at temperatures up to 1500°C. Test specimens were held on an anvil in the furnace and heated rapidly to the test temperature. An impacter broke the samples in 3-point bending, and high speed digital recorders stored the outputs of force and velocity transducers. The controlled flaw technique was utilized to obtain the critical stress intensity factor, K_{IC}. Hot-pressed silicon nitride materials containing MgO, CeO_2 or ZrO_2 sintering aids showed a decrease in K_{IC} as the temperature exceeded 1300°C. Hot-pressed silicon carbide containing alumina sintering aid showed a similar decrease. Sintered α-SiC, on the other hand, showed a gradual increase in K_{IC} at temperatures up to 1500°C. Reaction bonded SiC failed to break at the controlled flaw, but exhibited a drop in impact fracture force at temperatures approaching the melting point of silicon.

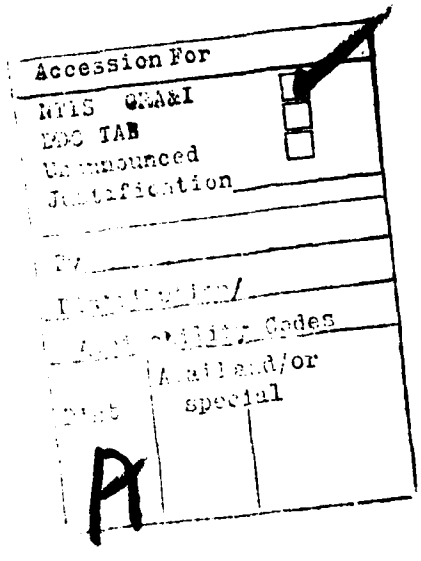

INTRODUCTION

Over the years, the need for an understanding of the high temperature impact fracture behavior of high performance ceramic materials has become apparent. The possibility of strain rate sensitivity of fracture strength and fracture toughness should be explored. The present program was designed to explore the high temperature impact behavior of silicon nitride and silicon carbide materials, using an instrumented impact testing apparatus in which the sample was maintained under isothermal conditions during the impact event. It also was planned originally to use the double torsion specimen to explore crack growth at high temperatures, but the available testing machine had too high a compliance to give reliable results.

The materials which were tested included commercially available and experimental hot-pressed Si_3N_4, commercially available hot-pressed and reaction sintered SiC, sintered α-SiC, an experimental reaction sintered SiC, and SiC-Si_3N_4 composites. It was originally planned to prepare sinterable SiC powder in a plasma reactor, since none could be obtained commercially, but it was determined that this would be infeasible.

EXPERIMENTAL METHODS

The impact apparatus is shown schematically in Fig. 1 of Appendix A. It was designed to overcome the major objection to most previous high temperature impact studies. Specimens in previous studies were subjected to thermal shock as they were removed from a furnace and placed on the anvil[1], or they contained temperature gradients as a result of being heated on the anvil by induction coils, flames, or by

direct heating by passage of electrical current through the specimen.[2] Kingery and Pappis[3] avoided thermal shock or gradients, but their specimens were subjected to repeated increasingly strong blows until failure occurred. However, the possibility of lowered apparent strength through impact fatigue[4] makes the results questionable. More recent attempts at instrumented impact studies at high temperature include a free-fall drop weight method[5] and a three-part furnace which rapidly opens as the impact hammer swings toward the specimen[6].

The instrument designed and built for the present study incorporates isothermal conditions and full instrumentation to measure force and velocity during the impact event at controlled impact velocities. The specimen rested within a small box furnace, heated with molybdenum disilicide heating elements*. Specimens were brought to temperature over a period of 0.25 to 1.5 hours and impacted in 3-point bending at impacter velocities of from 10 - 45 cm/s. A low compliance quartz load cell** was used to detect the force during impact, and the force signal was recorded in a high speed digital waveform recorder†. The velocity of the impact body was monitored by a velocity transducer‡, and the velocity signal was also stored on a digital recorder. The outputs of the recorders were displayed on an oscilloscope and on an X-Y recorder, and a punched paper tape was generated. The furnace in which most of

---

*Kanthal Corporation, Bethel, Connecticut.

**Kistler Instruments, Sunstrand Data Corp., Redmond, Washington.

†Biomation Corporation, Cupertino, California.

‡Trans-Tek, Inc., Ellington, Connecticut.

the work was completed was limited to 1400°C. A second furnace, capable of 1600°C, and an improved impacter system was constructed for testing the sintered α-SiC material.

The velocity of the impact head was controlled by a pulley system and pneumatic damper, the latter consisting of a metal piston traveling inside a metal cylinder closed at one end. Valves in the closed end were adjusted to control the amount of air flowing in behind the moving piston, and thus controlling the drop velocity. A retraction motor controlled by position microswitches withdrew the impact nose from the hot zone of the furnace in less than one second after impact. Thus the specimen was maintained completely isothermally during the impact event, and both the velocity and force during impact were recorded. We are not aware of another unit that has these capabilities.

A variety of specimens were prepared and tested. In order to gain experience with the apparatus and compare results with previous work, the first tests were run with a hot pressed Si_3N_4, namely, NC-132*.[7] Test bars, 34.5 mm long with a cross section of 3.0 x 3.0 mm, were cut from the hot-pressed billet and ground through 600 grit SiC powder on a 2-surface lap to insure parallelism of opposite faces. Grinding was continued until the cross sectional dimensions were constant along the length to within 0.03 mm. A surface finish of better than 20μ in. RMS was achieved. The controlled flaw technique[8,9], in which a Knoop diamond indenter is used to produce an elliptical flaw on the tensile surface of a beam loaded in 3-point bending, was used. The critical stress intensity factor, K_{IC}, was calculated from the dimensions of the flaw, the beam,

*Norton Company, Worcester, Massachusetts.

and the fracture load. Tests were completed at room temperature, 1100°, 1250°, and 1400°C, in air, at an impacter velocity of about 40 to 45 cm/s. Further details are recorded in Appendix A.

A commercially available hot-pressed SiC, NC-203*, was also evaluated in a similar fashion. Preliminary fracture toughness measurements were made at an impacter velocity of about 10 cm/s[10], and later at higher velocities employing faster heating.[11]

A commercially available reaction-sintered SiC, NC-435**, was tested, also by similar techniques.[11,12]

A number of externally prepared experimental materials were tested. These included hot-pressed silicon nitride doped with zirconia†, and ceria‡, sintered α-SiC⊕, and an experimental SIALON prepared in the present program.[7]

Plans to work with hot-pressed SiC were frustrated by unavailability of sinterable powder.

Reaction-sintered SiC was prepared using an organic precursor technique.[11-12] A 1500-grit SiC powder# was mixed with furfuryl alcohol, which was subsequently polymerized, pyrolized, and reacted with liquid Si.

The initial work followed the methods of Hucke[13], using furfuryl alcohol with or without admixtures of diethylene glycol as a pore-forming

---

*Norton Company, Worcester, Massachusetts.

**Norton Company, Worcester, Massachusetts.

†Harbison-Walker Refractories, Gerber Research Center, Pittsburgh, PA., courtesy of Dr. D. Petrack.

‡Naval Research Laboratories, Washington, D.C., courtesy of Dr. R. Rice.

⊕Carborundum Company, Niagara Falls, NY.

#Carborundum Company, Niagara Falls, NY.

agent. The furfuryl alcohol was polymerized with p-tolune sulfonic acid as a catalyst. While Hucke usually worked exclusively with organic materials, in the present work the organics were added to the α-SiC powder. In the latter part of the program, a surfactant was also added to provide better dispersion of the diethylene glycol in the furfuryl alcohol.

The typical procedure involved premixing the furfuryl alcohol and ethylene glycol, then adding the catalyst, and finally, the SiC powder. Formulations of 70 vol% SiC powder were then die-pressed and the polymerization of the furfuryl alcohol was subsequently allowed to proceed at 150°C. Alternatively, slurries of 30 vol% SiC were cast, polymerized and pyrolized.

Pyrolysis was accomplished during slow heating with the rate particularly slow in the range of the major exothermic peaks involving vaporization of the diethylene glycol and decomposition of the furfuryl alcohol resin. Maximum pyrolysis temperature was typically 900°-1000°C. The pyrolysis was conducted in flowing nitrogen gas to remove the products of pyrolysis. It was learned that the subsequent penetration of liquid silicon could be improved by heating the pyrolyzed samples to 1600°C in vacuum, which tended to open the pores in the amorphous carbon residue left by pyrolysis.

The final step involved placing the pyrolyzed and high temperature annealed specimens in contact with liquid Si and heating up to as high as 1800°C. The resulting specimens consisted of the pre-existing α-SiC, new β-SiC, and residual Si. It was observed that with the 30 vol% liquid specimens, dimensional stability was very good, with

about 2% linear shrinkage from the as-pressed condition to the siliconized final specimens.

Attempts to hot press SiC and composites of SiC and Si_3N_4 were frustrated through the lack of suitable sinterable SiC powder and also a serious failure of the hot press which rendered it useless for further work.

An attempt was made to prepare Si_3N_4-SiC-Si composites by impregnating silicon nitride* with a furfuryl alcohol-diethylene glycol mixture followed by polymerization, pyrolysis, and infiltration with silicon in the manner similar to the reaction sintered SiC methods discussed above. The SiC yield was increased by ad-mixing 4 vol% carbon black with the liquid mixture. Although considerable progress was made, the goal of a fully dense composite material was not realized before the termination of the grant, and no specimens were prepared for fracture studies.

RESULTS AND DISCUSSION

Silicon Nitride

The results of the investigation of hot-pressed silicon nitride, including NC-132 and experimental compositions, have been reported and are included as Appendix A and Appendix B. The most significant result observed was the 20% drop in K_{IC} at 1400°C compared with values at 1250°C and lower. This is in contrast to the rapid rise in K_{IC} at 1400° observed by others at much lower strain rates. This high strain rate sensitivity to K_{IC} is undoubtedly caused by the viscous intergranular phase resulting from the MgO sintering aid used in this material.

*AME Materials, Ltd., England.

The experimental ceria-doped and zirconia-doped silicon nitrides exhibited a higher K_{IC} than the NC-132, but showed a similar decline with temperature, as shown in Fig. 5 of Appendix B. The ceria-doped material showed the highest strength under impact loading of any of the Si_3N_4 materials tested.

The experimental SIALON material contained 80 wt% Si_3N_4* and 20 wt% aluminum oxide**. The powders were mixed in a vibratory mill and hot-pressed at 1700°C for 4 hours at 25,000 psi in flowing nitrogen. A density of 3.12 g/cm^3 was measured by immersion. The critical stress intensity factor was about 2.4 MN/m$^{3/2}$ at room temperature, but rose to about 6 from 1100°C to 1400°C.

Hot-Pressed Silicon Carbide

Because of the unavailability of sinterable silicon carbide powder, this part of the work was confined to commercial hot-pressed SiC, namely, NC-203†. This material has Al_2O_3 added as a densification aid, and consists largely of the 6H form of α-SiC. The density of the billet tested was 3.32 g/cm^3 and the average room temperature flexural strength was 790 MN/m^2, as reported by the supplier.

Test bars were ground on all sides with 10 μm and 5 μm boron carbide powder in a two-surface lapping machine. A 2600 g Knoop microhardness indentation was placed in the tensile surface of each test

*Controlled phase 85 300 mesh, Advanced Materials Engineering, Ltd.
**0.3 micron, 99.98%, A. Maller Company, Providence, Rhode Island.
†Norton Company, Worcester, Massachusetts.

bar, and the bars were broken at 800°, 1000°, 1200°, and 1400°C in air at an impact velocity of about 19 cm/s at elevated temperatures, and about 10 cm/s at room temperature.

There was no trace of non-catastrophic crack growth for any specimen broken at any temperature. The load trace dropped sharply to zero within 15 μs after fracture initiation. This behavior agrees with the slow bend tests reported in the literature.

The value of K_{IC} was uniformly higher by about 30% than the data reported on slow bend tests, reaching a maximum value of about 5 $MN/m^{3/2}$ at 1000°-1200°C.[10] It turned out that this effect was probably due to oxidation during a rather slow (1.5 hr) heat-up schedule. Later specimens that were heated more rapidly did not show this elevated K_{IC}.[11] However, the slow bend tests and both rapidly heated and slowly heated specimens showed K_{IC} values, which were lower at 1400° than at 1200°C, probably due to the influence of the intergranular phase brought about by the Al_2O_3 sintering aid.

Sintering α-Silicon Carbide

A supply of 1/8" square by 1.5" long polished test bars of sintered α-SiC was acquired.* These were tested with the controlled flaw technique at room temperature, 1000°, 1200°, 1350°, and 1500°C at impact velocities on the order of 15 cm/s.[12] The heating rate at elevated temperatures was rapid, with the fracture temperature being achieved in the order of 15 - 25 minutes. The values of K_{IC} averaged 3.4 at room temperature, 3.3 at 1000°, 4.9 at 1200°, 4.7 at 1350°, and 5.0 $MN/m^{3/2}$ at 1500°C. All fractures were completely brittle, with no

*Carborundum Company, Niagara Falls, New York.

evidence of subcritical crack growth. Data analysis for this material is still in progress; a preprint will be supplied as quickly as one becomes available.

Reaction-Sintered Silicon Carbide

The materials tested included commercially available material, NC-435*, and experimental materials prepared as part of the present program.

Specimens were cut from the commercial as well as the experimental materials, and surface flaws were introduced by a Knoop indenter under 2600 g load. However, it was discovered that the specimens did not break at the flaw at elevated temperatures, indicating that the flaw was healed, so subsequent measurements were made without controlled flaws.

The microstructure of the experimental material was significantly improved over the NC-435.[11] The latter showed a larger volume fraction of silicon phase, and moreover, a coarser silicon "particle" size. In addition, the volume fraction and coarseness of the structure changed from the interior relative to the surface of the specimens. In the present material, the "particle" size of the silicon phase was much smaller and the volume fraction much less, being on the order of 9 to 24%, depending upon the amount of diethylene glycol in the polymer mix. The best of the present materials showed no measurable open porosity, and less than 1% total porosity.

Specimens were cut from the material and tested at temperatures

*Norton Company, Worcester, Massachusetts.

up to 1400°C at an impact velocity of about 33 cm/s. Because the samples did not break at the flaw, the impact flexural strength was obtained, rather than K_{IC}. NC-435 showed a value of 190 MN/m^{-2} at room temperature, with values of 300 at 1000° and 1200°C, 434 at 1300°C, and 135 at 1400°C at an impact velocity of about 38 cm/s. The new material showed a similar trend,with temperature, but somewhat higher values.

EVALUATION OF IMPACT APPARATUS

The apparatus developed for this study has successfully overcome the major objections of previous high temperature impact testing methods. It provides for the sample being under isothermal conditions at the moment of impact, with no temperature gradients or temperature transients to influence the results. The design is relatively simple, reliable, and rugged. The use of molybdenum disilicide heating elements and an adequate power supply makes it possible to heat specimens to the impact temperature in 15-20 minutes. Temperatures as high as 1650° have been reached, but the heating elements began to sag. The practical limit of the apparatus is 1600°C.

Through the use of force and velocity transducers, both the load exerted on the specimen and the velocity of impact are measured continuously during the impact event. This allows for determination of the load-deflection curve, as well as the fracture stress as a function of impact velocity. Through the use of the controlled flaw technique, the stress intensity factor, K_{IC}, can be calculated from the fracture force, beam geometry and flaw geometry.

The impact velocity can be varied from less than 10 cm/s to about 100 cm/s. However, at higher impact rates, in common with stan-

dard instrumented Charpy tests of brittle materials,[14] oscillations in load are observed during the specimen loading. Silicon nitride materials showed minimum oscillations at less than 50 cm/s, while SiC materials showed oscillations unless the impact velocity was reduced to less than about 30 cm/s. These oscillations, if not too extreme, tend to damp out before the fracture event.

In summary, it is felt that the present apparatus provides a convenient method of impact testing of small specimens at temperatures up to 1600°C, and impact velocities from 5 to 100 cm/s.

References

1. J. J. Brennan and M. A. Decrescente, Report M911294-4, United Aircraft Research Laboratories (1973).
2. H. C. Chandan, H. Abe, and R. C. Bradt, Ceram. Bul. 56 [3] 289 (1977).
3. W. D. Kingery and J. Pappis, J. Am. Ceram. Soc., 39, 64 (1956).
4. B. K. Sarkar and T.G.J. Glinn, J. Mater. Sci., 4 [11] 951 (1969).
5. James Wimmer, Air Force Materials Lab., AFML-7R-76-56, February 1976.
6. C. O. Hulse and G. A. Peterson, Ceram. Bul., 56, 289 (1977).
7. Stephen T. Gonczy, Ph.D. Thesis, Northwestern University, 1978.
8. J. J. Petrovic, L. A. Jacobson, P. K. Talty, and A. K. Vasudevan, J. Am. Ceram. Soc. 58 [3-4] 113-16 (1975).
9. J. J. Petrovic and L. A. Jacobson, J. Am. Ceram. Soc. 59 [1-2] 34-37 (1976).
10. Daniel T. Hung, M.S. Thesis, Northwestern University, 1978.
11. Jeffrey Suh-Sun Wang, Ph.D. Thesis, Northwestern University, in preparation.
12. Paul G. Lindquist, M.S. Thesis, Northwestern University, in preparation.
13. E. E. Hucke, U.S. Patent 3,859,421, Ger. Offen. 2,326,937,101, pp.(1975).
14. R. L. Bertolotti, J. Am. Ceram. Soc. 57, 300 (1974).

LIST OF PUBLICATIONS

1. Stephen T. Gonczy and D. Lynn Johnson, "Impact Fracture of Ceramics at High Temperature", Fracture Mechanics of Sintering, Vol. 3, eds. R. C. Bradt, D.P.H. Hasselman and F. F. Lange, Plenum Press, N.Y. (1978), pp. 495-506.

2. Stephen T. Gonczy and D. Lynn Johnson, "High Temperature Impact Fracture of Si_3N_4", to be submitted to the Journal of the American Ceramic Society.

DISSERTATIONS

1. "The Effect of Various Densifying Agents Upon the High Temperature Impact Strength of Hot-Pressed Silicon Nitride", Stephen T. Gonczy, Ph.D. awarded August 1978.

2. "Instrumented High Temperature Impact Test of SiC", Daniel T. Hung, M.S. awarded June 1978.

3. Jeffrey S. Wang, Ph.D. thesis in preparation.

4. Paul G. Lindquist, M.S. thesis in preparation.

LIST OF PROFESSIONAL PERSONNEL WHO PARTICIPATED IN THE RESEARCH

Principal Investigator

D. Lynn Johnson, Professor of Materials Science & Engineering

Post-Doctoral Research Associates

Emilija Kostić, 3/29/78-3/31/79

Shu-ichi Takeda, 4/1/79-9/30/79

Graduate Students

Stephen T. Gonczy - Completed Ph.D. August 1978.

Daniel T. Hung - Completed M.S. June 1978.

Jeffrey S. Wang

Paul G. Lindquist

Secretary

Wilma Hackl (½ time)

APPENDIX A

Fracture Mechanics of Sintering, Vol. 3, eds. R. C. Bradt, D.P.H. Hasselman and F. F. Lange, Plenum Press, N.Y. (1978).

IMPACT FRACTURE OF CERAMICS AT HIGH TEMPERATURE

Stephen T. Gonczy and D. Lynn Johnson

Department of Materials Science and Engineering
Northwestern University
Evanston, Illinois 60201

ABSTRACT

Samples of hot-pressed silicon nitride were tested in 3-point bend impact loading at ambient temperature, 1100°C, 1250°C, and 1400°C under isothermal conditions. Dynamic stress intensity factors (K_{IC}) were calculated from the fracture load and the dimensions of an induced surface flaw, produced by a Knoop hardness indenter. Dynamic stress intensities of about 5.25 $MN/m^{3/2}$ were determined for all temperatures up to 1250°C. A 20% drop in K_{IC} was found at 1400°C. This drop in K_{IC} coincides with a change in the fracture surface at the same temperature, indicating a change in the micromechanics of fracture at 1400°C.

I. INTRODUCTION

The use of ceramics as structural components requires a knowledge of their impact properties at ambient and high temperatures. Impact studies on alumina[1], silicon carbide[2,3,4], and silicon nitride[4,5] have been done with instrumented Charpy or drop-weight tests. The Charpy-type tests at high temperatures have been limited by the fact that the specimens have been fractured under transient thermal conditions, or at least with thermal gradients along and through the specimens. The free-fall drop-weight test fractures the specimen under isothermal conditions; the instrumentation measures the deflection of the specimen, rather than the load exerted on the specimen.[4,5]

Recent studies by several investigators[6,7,8] have analyzed the use of a controlled semi-elliptical surface flaw induced on the

tensile side of a ceramic slow bend specimen by a Knoop hardness indenter with a 2½ kg load. The shape and dimensions of the flaw produced by a given load are reproducible. In accordance with fracture theory, the flaw reduces the bend strength of the specimen. The use of the induced flaw reduces the scatter of the bend strengths, normally found among unflawed specimens, caused by the statistical distribution of natural flaws.[6] Additionally, the critical stress intensity factor, K_{IC}, can be evaluated by using the induced flaw dimensions.

The present investigation was designed to take advantage of the controlled surface flaws and to break the specimens at controlled impact rates under isothermal conditions.

II. EXPERIMENTAL PROCEDURE

Hot-pressed silicon nitride* was cut into test bars 34.5 mm long with a cross section of 3.0 by 3.0 mm. These bars were polished on all sides with 600 grit SiC powder on a two-surface lapping machine. Polishing continued until all visible surface imperfections were eliminated and until the cross-sectional dimensions were constant along the length to within .03 mm. A surface finish of better than 20 μinches RMS was achieved.

Using a microhardness tester with a Knoop diamond indenter, an indentation was centered on the tensile side of each test bar. The long axis of the indentation was perpendicular to the tensile stress direction; its length was measured with an optical microscope.

Three-point bend impact loading of the test bars was done at room temperature, 1100°C, 1250°C, and 1400°C in air in a test system shown schematically in Fig. 1. The tensile stresses were in a plane perpendicular to the hot-pressing direction of the material. The test beams were held in a notched alumina tube with a bending span of 29.0 mm in a furnace heated by molybdenum disilicide resistance heating elements. The temperature was monitored by a thermocouple placed ≈10 mm directly above the center of the beam. Test bars were taken from room temperature to test temperature over a period of 1½ hours.

The velocity of the impact head was controlled by a pulley system and pneumatic damper, consisting of a metal piston traveling inside a metal cylinder closed at one end. Valves in the closed end were adjusted to control the amount of air flowing in behind the moving piston, and thus controlling the drop velocity.

*NC-132, Norton Co., Worcester, MA.

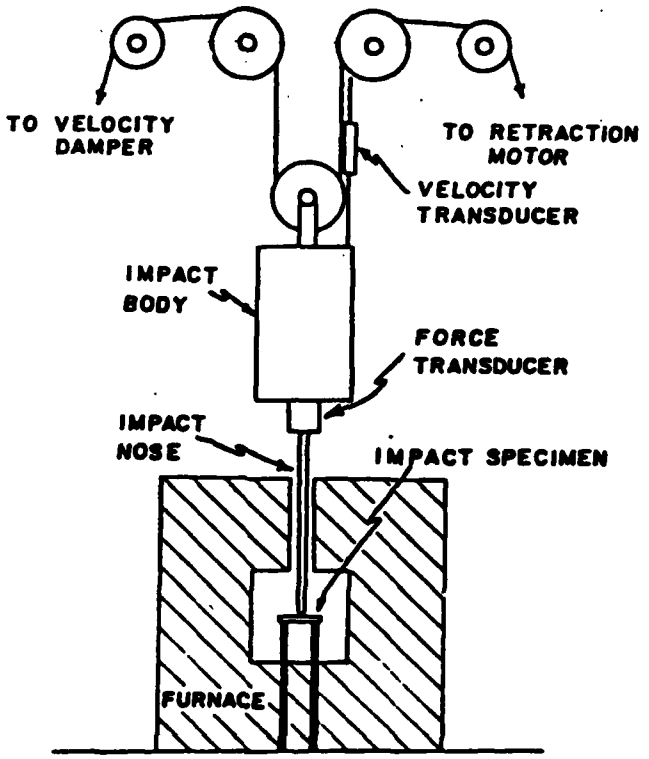

Figure 1. Schematic Diagram of Impact System and Furance.

A retraction motor controlled by position microswitches withdraws the impact nose from the hot zone of the furnace after fracture occurs. The impact nose enters and leaves the furnace over a period of less than one second. The impact body is kept aligned with the specimen by guides at the top and bottom of the drop path.

A quartz load transducer*, located between the impact nose and the impact body, monitors the force applied to the test beam. The velocity of the impact body is monitored by a velocity transducer.†

---

*Kistler Instruments, Sundstrand Data Corp., Redmond, WA.

†Trans-Tek Inc., Ellington, CT.

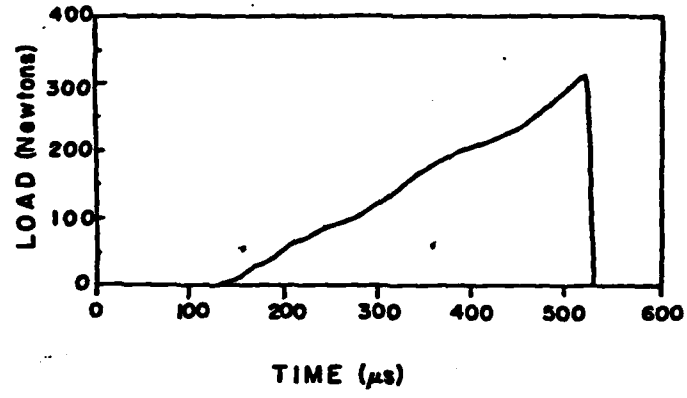

Figure 2. Typical Load-Time Trac. for Impact Velocity of 45 cm/s.

The mass of the impact body is 2 kg and is made of brass. The impact nose is made of a titanium alloy and is 7.5 mm in diameter.

A charge amplifier* is used to condition the force signal. Two high speed digital waveform recorders** store the two signals. The recorder used for the load signal has 2048 units of 8-bit memory to record events as short as 409 μs. The recorder used for the velocity signal has 256 units of 6-bit memory to record events as short as 25.6 μs. Both recorders are triggered by the rise of the load signal to a specified trigger level. The recorders are operated in a pretrigger mode, which inusres the recording of that portion of the signal prior to the point at which the recorder is triggered.

The recorders have both digital and analog outputs. The stored signals can be observed on an oscilloscope, transferred to a strip chart recorder for hard analog copy, and transferred to a Teletype punch unit for hard digital copy.

A typical graph of the load signal for an impact fracture is shown in Fig. 2. A graph of the corresponding velocity signal is shown in Fig. 3.

Fracture surfaces were studied by optical microscope using both polarized and unpolarized light. The surfaces were examined

*Kistler Instruments, Sundstrand Data Corp., Redmond, WA.
**Biomation Corp., Cupertino, CA.

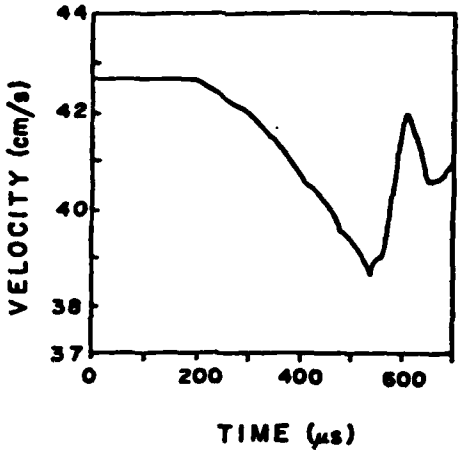

Figure 3. Typical Velocity-Time Trace for Impact Velocity of 45 cm/s.

primarily for characterization of the fracture surface and for measurement of the depth of the induced flaw.

III. CALCULATION OF K_{IC}

The Knoop hardness indenter introduces a semi-elliptical surface crack on the tensile side of the bend specimen. This surface flaw will grow catastrophically when the stress intensity at the flaw reaches a critical value. According to fracture mechanics theory, the stress intensity factor for a semi-elliptical surface flaw in bending is given by:[6,9]

$$K_I = \sigma M (\pi a/Q)^{\frac{1}{2}} \quad (1)$$

where σ is the maximum outer fiber tensile stress, M is a numerical factor related to flaw and beam geometry, a is the flaw depth, and Q is given by:[6,9]

$$Q = \Phi^2 - 0.212 (\sigma/\sigma_{ys})^2 \quad (2)$$

where σ_{ys} is the tensile yield stress and $0.212 (\sigma/\sigma_{ys})^2$ is a plastic zone correction factor. At the loading rates used in this work,

this plastic correction factor is considered negligible. The value Φ is the elliptical integral[9]

$$\Phi = \int_0^{\pi/2} \left[1 - \frac{c^2 - a^2}{c^2} \sin^2 \theta\right]^{\frac{1}{2}} d\theta \qquad (3)$$

which is tabulated in standard mathematical tables; c is the major axis of the flaw.

The value for M was taken as 1.03 based upon bend tests by Petrovic et al[6] of silicon nitride with similar beam and flaw geometry.

IV. RESULTS AND DISCUSSION

Analysis of the Load-Time and Velocity-Time Traces

A study of the load-time traces shows that the average time between the points of initial loading and fracture was approximately 325 μs for all specimens broken with an impact velocity in the 40-45 cm/s range. The magnitude of the fracture load for all the specimens was in the range of 300 N and depended upon the cross-sectional geometry of individual beams.

The shape of the load-time traces was generally of the form shown in Fig. 2. Small scale oscillations were seen in some cases. These oscillations, superimposed on the linear load trace, had a wavelength of 30-40 μs and a magnitude of less than 10% of the final fracture load. These oscillations are most likely caused by vibration of the test beam itself under inertial loading. A second explanation is stress wave reflections between the tip of the impact nose and the junction of the impact nose with the load transducer.

There was no sign of non-catastrophic crack growth for any specimens broken at any temperature. The load trace dropped sharply to zero within 10 μs after fracture initiation.

The velocity curves were of the form seen in Fig. 3. Impact velocities were not precisely reproducible between tests, but ranged between 41 and 45 cm/s. The drops in velocity that occurred with impact were generally linear, and the duration of the linear portion agreed within ±10% of the duration of the corresponding load trace. The fact that the velocity transducer is attached to the upper part of the impact body explains the discrepancies. The transducer monitors the velocity of the impact body, rather than

the precise velocity of the impact nose.

Fracture Surfaces and Flaw Size Analysis

The fracture surfaces of all the broken specimens had regions described by Kirchner[10] as mirror, mist, and hackle. The mirror is a region of smooth flat surface. It is surrounded by mist, which is less reflective and stippled. The mist is bordered by hackle, which is characterized by a rough region of hills and valleys. For all specimens the location of the mirror region proved conclusively that the Knoop flaw was the point at which fracture started.

The fracture surfaces of specimens broken at room temperature, 1100°C, and 1250°C were all similar, showing mirror, mist and hackle. The relative amounts of each region were not markedly different between the different temperatures. However, on the specimens broken at 1400°C virtually no hackle was seen, and the mist region was smoother and more homogeneous. This change in fracture surface at 1400°C is a possible indication of a change in the mode of fracture propagation; it coincides with the 20% decrease in critical stress intensity observed at 1400°C.

A polarizing microscope was used to measure the depth of the crack beneath the Knoop flaw. The general location of the flaw on the fracture surface was known from both the original positioning of the diamond indenter and the location of the mirror region on the fracture surface. However, in only 45% of the 27 specimens broken could the flaw depth be identified and measured with certainty. In 33% of the specimens the flaw could be observed and measured with only a fair degree of accuracy. In 22% the flaw could not be identified at all. This difficulty in identification and measurement was partially caused by oxidation of the fracture surface after fracture. There was also pick-up of alumina fiber furnace insulation, when the specimen struck the furnace walls while rebounding from the impact nose. In some cases the oxidation and alumina totally obscured the portion of the test beam on which the Knoop flaw was located.

The flaw itself, even when the fracture surface was clean, was not always identifiable under either polarized light or unpolarized light. On other specimens the flaw was easily located and measured; all identifiable flaws were clearly elliptical in shape. Figure 4 shows the average flaw dimensions for Knoop indentation loads of 2 kg and 2½ kg. Similar data from Petrovic et al[6] for NC-132 silicon nitride is in good agreement.

For those specimens broken at high temperature, there was no sign of slow crack growth. All identifiable Knoop flaws were of

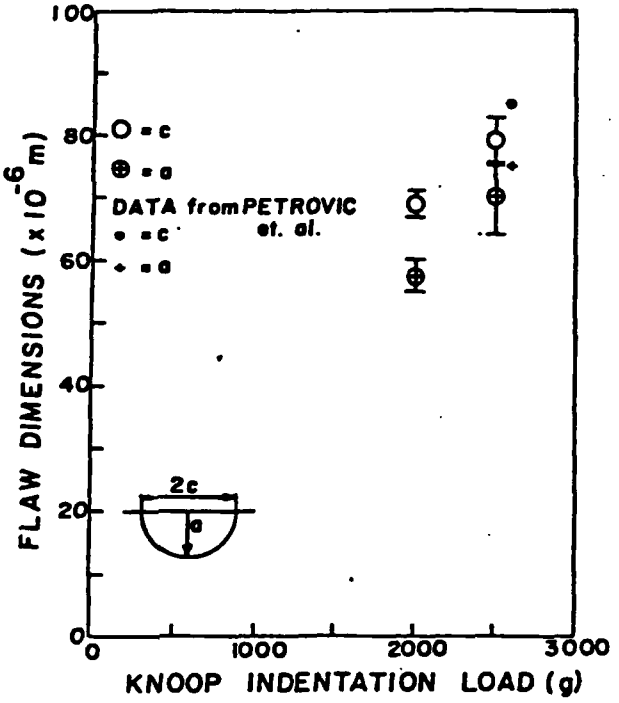

Figure 4. Flaw Dimensions vs Knoop Load for NC-132 Silicon Nitride (Error Bars Indicate Standard Deviation)

the same general dimensions as the flaws on the specimens broken at room temperature. Petrovic observed in his bend tests of HS-130 silicon nitride that the flaw grew at all tests above 1200°C using a cross-head speed of .01 cm/min. On tests at 1300°C the flaw grew approximately 10 times its initial size before catastrophic failure. They also noted that at 1300°C the amount of slow crack growth decreased with increasing cross-head speed. The fastest cross-head speed used by Petrovic et al was .5 cm/min. With the present impact velocity of about 2500 cm/min, the lack of any signs of slow crack growth at high temperatures is consistent with theory.

The fracture surfaces showed no sign of Hertzian-type damage. In many cases, however, there was secondary cracking on the flawed side of the specimen. No study was made of the character or causes of these secondary cracks.

Calculation of K_{IC} Factors

The bending stress at fracture and the measured flaw depth were used in K_{IC} calculations. When the flaw could not be identified or accurately measured, an expected value for the flaw depth was interpolated from the measured flaw length on the surface and the average flaw depth/flaw length ratio determined among all specimens. This interpolated value was then used to determine K_{IC}.

Room Temperature K_{IC}

Petrovic et al[6] showed that the room temperature strength and K_{IC} values for flawed HS-130 Si_3N_4 specimens could be increased 30% by annealing the flawed specimens at over 1100°C in air for 6 hours. They attributed this increase to the elimination of residual stresses at the flaw site; the plastic deformation caused by the diamond indenter leaves the immediate area in a compressive state. This plastically strained region acts as a wedge in the crack, placing the crack tip in a tensile stress state. This residual tensile stress acts with any applied stress, and thus reduces the amount of applied stress needed to reach a critical stress level. Annealing the specimen eliminates this residual stress.

Specimens of NC-132 with flaws were tested at room temperature in two conditions. One set of specimens was tested in an unannealed condition, while a second set was annealed in air for 4 hours at 1100°C. The K_{IC} values for both sets are shown in Fig. 5. The 30% increase in K_{IC} values for the annealed specimens is in agreement with Petrovic et al. The K_{IC} values at room temperature for the annealed specimens are also in agreement with dynamic stress intensity measurements of HS-130 silicon nitride conducted at impact velocities of 1.3×10^4 cm/min by Mendiratta, Wimmer, and Bransky.[5]

High Temperature K_{IC}

This study tested the NC-132 specimens at 1100°C, 1250°C, and 1400°C. The computed critical stress intensity values are shown in Fig. 5. The K_{IC} values for the annealed specimens tested at room temperature and the values for unannealed specimens tested at 1100°C and 1250°C are constant near 5.25 $MN/m^{3/2}$. These values are slightly higher than the K_{IC} values determined at similar temperatures by Evans and Wiederhorn[11] in double torsion and by Petrovic et al[6] in 4-point bend for HS-130 Si_3N_4.

The data in the room temperature to 1250°C range also agrees with impact K_{IC} data by Mendiratta et al.[5] They tested HS-130 with induced surface flaws. The impact velocity in that study was an order of magnitude larger than this study; but the difference in

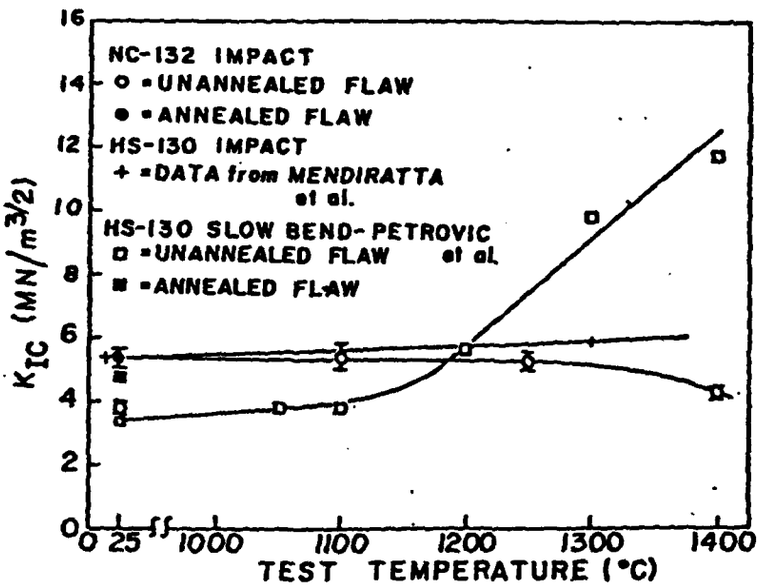

Figure 5. K_{IC} versus Temperature for Silicon Nitride (Error Bars Indicate Standard Deviation)

velocities is not apparent in the K_{IC} values.

In tests at 1400°C the K_{IC} value dropped 20% to 4.25 MN/m$^{3/2}$. This is in marked contrast to the high temperature double torsion and slow-bend data for HS-130. In those studies the K_{IC} value increased by a factor of 3. But this increase was caused by slow crack growth. The researchers determined K_{IC} using the flaw depth marked by the onset of catastrophic fracture. As Petrovic et al pointed out, the depth dimension increased at 1300°C by a factor of 10 by the slow crack growth mechanism.

At the faster loading rates characteristic of impact, this slow crack growth does not have time to occur. The flaw does not grow, and the critical stress intensity does not increase. Mendiratta et al tested their samples at a maximum temperature of 1300°C and saw little change in K_{IC} values compared to room temperature values.

Thus the drop in K_{IC} values for Si_3N_4 at 1400°C under impact loading has not been observed prior to this study. However, a

drop in K_{IC} at high temperatures under slow-bend testing was observed by Petrovic et al[7] in studies of hot-pressed silicon carbide. In that study silicon carbide, unlike silicon nitride, showed no signs of slow crack growth, even at the highest test temperature of 1400°C. Petrovic and Jacobson theorized that the drop in K_{IC} for silicon carbide at high temperatures was caused by a change in the micromechanism of the fracture process. There was a marked difference between SEM micrographs of the fracture surfaces broken at 1400°C in vacuum and at room temperature in air. They also theorized that a grain boundary phase rich in impurities provided an easier path for brittle fracture at high temperatures.

This same theory is a possible explanation for the drop in K_{IC} for silicon nitride at 1400°C under impact loading. The difference in fracture surfaces noticed between samples broken at 1250°C and at 1400°C adds credence to this theory. A grain boundary phase containing the hot-pressing additives is often cited as the source of the grain boundary sliding which contributes to the slow crack growth occurring over 1200°C. If at 1400°C this grain boundary region becomes significantly less viscous and much weaker, it will provide an easier path for brittle fracture; and this would cause a marked decrease in high-temperature strength even under impact load.

V. CONCLUSIONS

The controlled surface flaw technique used for slow bend tests is also applicable to impact loading tests of ceramics. Using the impact fracture load and the measured flaw dimensions, the dynamic stress intensity factors can be determined.

Impact tests of NC-132 silicon nitride at high temperatures show no sign of the slow crack growth seen in 4-point bend studies at similar temperatures.

The fracture surfaces of the NC-132 impact specimens show definable areas of the fracture regions of mirror, mist, and hackle.

Room temperature impact K_{IC} values for the flawed NC-132 can be raised by annealing the specimen in air at 1100°C.

The impact K_{IC} values in the region of ambient temperature up to 1250°C show a consistent value of roughly 5.25 $MN/m^{3/2}$ for NC-132 silicon nitride.

There is a marked decrease of 20% in the impact K_{IC} of NC-132 at 1400°C. This decrease correlates with a change in fracture surface, compared with specimens broken at 1250°C or less. This indicates a change in the micromechanism of fracture at this tem-

perature level. Thus the impact resistance of NC-132 silicon nitride is not constant beyond 1300°C, but drops. This indicates a temperature limitation for NC-132 in its consideration for high-temperature gas turbines.

ACKNOWLEDGEMENT

The research upon which this work is based was supported by the Air Force Office of Scientific Research, Grant #AFOSR-76-2920-A.

REFERENCES

1. R. L. Bertolotti, "Strength and Absorbed Energy in Instrumented Impact Tests of Polycrystalline Al_2O_3", J. Am. Ceram. Soc. 57 [7] 300 (1974).
2. H. Abe, "Instrumented Charpy Impact Testing of Silicon Carbide", PhD Dissertation, Pennsylvania State University, May 1976.
3. H. C. Chandan, H. Abe, and R. C. Bradt, "Elevated Temperature Charpy Impact Test of Silicon Carbide", Abstract, Am. Ceram. Soc. Bul. 56 [3] 289 (1977).
4. J. M. Wimmer, I. Bransky, "Impact Resistance of Structural Ceramics", Am. Ceram. Soc. Bul. 56 [6] 552 (1977).
5. M. G. Mendiratta, J. Wimmer, I. Bransky, "Dynamic K_{IC} & Dynamic Flexural Strength of HS-130 Si_3N_4", J. Mat. Sci. 12 212 (1977).
6. J. J. Petrovic, L. A. Jacobson, P. K. Talty, and A. K. Vasudevan, "Controlled Surface Flaws in Hot-Pressed Si_3N_4", J. Am. Ceram. Soc. 58 [3-4] 113 (1975).
7. J. J. Petrovic, L. A. Jacobson, "Controlled Surface Flaws in Hot-Pressed SiC", J. Am. Ceram. Soc. 59 [1-2] 34 (1976).
8. Y. W. Mai, "Thermal Shock Resistance and Fracture Strength Behavior of Two Tool Carbides", J. Am. Ceram. Soc. 59 [11-12] 491 (1976).
9. G. R. Marrs and C. W. Smith, "A Study of Local Stresses Near Surface Flaws in Bending Fields", p. 23 in Stress Analysis and Growth of Cracks, Am. Soc. of Test. Mat., Spec. Tech Publ. #513, 1972.
10. H. P. Kirchner, R. M. Gruever, and W. A. Sotter, "Use of Fracture Mirrors to Interpret Impact Fractures in Brittle Materials" J. Am. Ceram. Soc. 58 [5-6] 188 (1975).
11. A. G. Evans and S. M. Wiederhorn, "Crack Propagation and Failure Prediction in Silicon Nitride at Elevated Temperatures", J. Mat. Sci. 9 [2] 270 (1974).

APPENDIX B

HIGH TEMPERATURE IMPACT FRACTURE OF Si_3N_4

by

Stephen T. Gonczy* and D. Lynn Johnson
Department of Materials Science and Engineering
Northwestern University
Evanston, Illinois 60201

ABSTRACT

*Currently with UOP Corporate Research Laboratory, Des Plaines, Illinois 60016

I. INTRODUCTION

The use of hot-pressed silicon nitride (HPSN) in structural components requires a knowledge of the ceramic's mechanical properties across a wide range of temperatures and loading conditions. Research on high temperature strength[1,2] and creep resistance[3,4] of HPSN has shown that the densifying agent (MgO, Y_2O_3, CeO_2, Al_2O_3, etc.) used in hot-pressing dramatically affects the high temperature strength properties. These densifying agents determine the character of the grain boundary phase. Softening of the grain boundary phase at high temperatures is cited[3,5,6] as the source of the grain boundary sliding, which is the proposed deformation mechanism above 1200°C in both slow bend and creep tests. The question of how the grain boundaries of HPSN react at high temperatures to the high loading rates of mechanical impact and thermal shock is important from both an engineering and a theoretical viewpoint.

There is published work on impact tests of silicon nitride densified with magnesia.[7,8] This research effort extended the high temperatures impact studies to HPSN densified with ceria and zirconia as compared to commercial HPSN (NC-132). Test bars of each type of HPSN were impact loaded in three-point bend under isothermal conditions at room temperature, 1100°C, 1250°C, 1325°C, and 1400°C. The use of the controlled Knoop-flaw technique[9,10] permitted the calculation of critical stress intensity (K_{IC}) factors for each test condition.

II. EXPERIMENTAL

A. Materials

Three different types of HPSN were obtained: a commercial magnesia-

doped HPSN* with a density of 3.28 g/cm^3, an experimental zirconia-doped HPSN** (designated Z-HPSN), and an experimental ceria-doped HPSN† (designated C-HPSN). The experimental Z-HPSN contained 8 w/o monoclinic ZrO_2 and had a density of 3.22 g/cm^3, with 0.8% open porosity. The experimental C-HPSN contained $\approx$ 10 w/o CeO_2 and had a density of 3.32 g/cm^3 with a 0.6% open porosity. Specific information on the composition and hot-pressing parameters of the NC-132 and the C-HPSN were proprietary. The composition and hot-pressing of the Z-HPSN were similar to other Z-HPSN billets described by Rice & McDonough.[11]

Test bars (34.5 mm long and 3.0 mm by 3.3 mm in cross section) were cut with a diamond slicing wheel from each HPSN billet. The bars were then successively surface lapped with a 240 mesh and a 600 mesh SiC/water slurry. The final surface finish was better than 20 RMS surface roughness by stylus measurement.

The test bars were indented with a Knoop hardness indenter on the plane perpendicular to the hot-pressing direction using a microhardness tester‡ with a micrometer stage and a controlled loading sequence (load, hold for 20 seconds, release). A 2500 gram load was used for 90% of all tested specimens. The indented flaw was oriented so the long axis was perpendicular to the length of the test bar. The length was measured with the graduated optical microscope on the microhardness tester.

---

*NC-132, Material Ref. # H292949A3848, Norton Co., Worcester, MA.

**Harbison-Walker Refractories, Gerber Research Center, Pittsburgh, PA. Courtesy of Dr. D. Petrack.

†Billet SIN VH3-119, Naval Research Laboratories, Washington, D.C., Courtesy of Mr. R. Rice.

‡TIKON Tester, Wilson Mechanical Instrument Div., American Chain & Cable, New York, NY.

B. Test Procedure and Test System.

Three-point bend impact loading of the test bars was done isothermally in air at room temperature, 1100°, 1250°, 1325°, and 1400°C. Tensile stresses in the test bar were in a plane perpendicular to the hot-pressing direction of the HPSN. The test bar temperature was measured by a thermocouple 10 mm from the center of the bar just prior to impact. The test furnace was heated with molybdenum disilicide resistance elements, with a heat-up time of 30-45 minutes.

The impact load was applied by a drop-weight impact fixture falling at a controlled velocity (45 cm/s). Stress rates for all tests were on the order of 10^6 MN/m^{2}s. The test bar was broken in the furnace, as the nose of the impact fixture entered through a ½" hold in the furnace roof. Test bars were not subjected to significant thermal variations spatially or chronologically during impact fracture. This was in contrast to instrumented Charpy tests with clam-shell furnaces or gas burners for heating.

The impact fixture was fitted with a quartz peizoelectric load transducer and a velocity transducer. Load and velocity signals were recorded by two high-speed digital waveform recorders. The impact test system with instrumentation was discussed in more detail in an earlier publication.[12]

C. Annealing Procedure.

A number of test bars were annealed after the Knoop flaw was introduced. This annealing was done between 700°C and 1100°C. The test bars were furnace cooled and fractured at room temperature. Specimens were annealed in either air or a nitrogen-hydrogen mix (0.1% H_2). The

furnace used for air annealing was a box furnace with silicon carbide heating elements. The nitrogen/hydrogen anneal was done in a closed tube furnace with silicon carbide heating elements. Both furnaces were proportionally controlled within $\pm 10^{\circ}C$ as measured by an independent thermocouple.

D. Fracture Surface Examination.

Both a stereoscopic microscope and a reflected light polarizing microscope were used to examine the fracture surface and the fracture flaw of each test bar. The stereoscopic microscope was used at 20X to examine the general fracture surface and to locate the fracture flaw at 50X. For accurate flaw measurement, a reflected light microscope was used with a calibrated filar eyepiece at 300X.

The time involved in specimen preparation and observation and the economic costs of equipment time prevented a scanning electron microscope (SEM) study of all 145 fracture specimens. However, one specimen from each group of specimens tested at a particular temperature was prepared and analyzed with the SEM*. The fracture surface was examined at ≈1000X and ≈5000X close to the fracture source, looking for evidence of intergranular and transgranular fracture. The tensile surface of the test bar was also examined in the SEM at ≈2000X. Here the surface was studied for the surface finish after final grinding and for oxidation of the tensile surface during annealing or high temperature testing.

III. RESULTS AND DISCUSSION

A. Character of Load-Time Trace.

A typical load-time trace is given in Figure 1. The traces for all

*Model S4, Kent Cambridge Instruments, Cambridge, England.

the tests showed a range of loading times (Point A to Point B in Fig. 1) of 200 to 600 microseconds and a range of fracture loads of 100 to 600 Newtons. The magnitude of the loading time and fracture load for each test bar depended on the bend strength and cross section geometry of the individual test bar. The shape of the load-time traces between Point A and Point B were generally linear. In many cases small scale oscillations were observed with a wavelength of 25 to 50 microseconds and a magnitude of less than 10% of the final fracture load. The most likely source of these oscillations would be vibration of the test beam itself under the initial impact loading. A calculation of the natural frequency of vibration for a supported beam and a free beam at room temperature with the characteristics of HPSN gave 1st and 2nd harmonics which bracketed the frequencies of the observed oscillations. A study of other vibrations sources such as stress wave reflection in the test bar or in the impact nose gave vibration frequencies which were significantly smaller or longer than the observed oscillations.

In all tests the load-time trace showed no indication of slow crack growth in the form of a load plateau or a gradual drop in load. The drop in load at fracture (Point C in Fig. 1) was consistently 10 to 15 microseconds in duration. That 10 microsecond duration was identical to the response time of the quartz load cell and the associated electronics.

B. Flaw Measurement and Evaluation.

The Knoop flaws on the NC-132 were identified and measured with the reflected light microscope. Flaw data are given in Table I. It was difficult to identify the flaws on some specimens tested at 1250°C or higher because of oxidation of the fracture surface after fracture. All

flaws were semi-elliptical in shape and all these specimens fractured at the flaw. The range of flaw dimensions on NC-132 as a function of Knoop load is shown in Fig. 2. The dimensions of Knoop flaws in NC-132 from Petrovic et al.[9] are in good agreement with those observed in this study.

In measuring the flaw dimensions on the NC-132 test bars fractured at successively higher temperatures, the data show no increase in measured flaw depth or width with increasing test temperature. This is in marked contrast to the work in slow bend tests of HS-130 HPSN by Petrovic et al.[9]. They observed crack growth in all tests above 1200°C; at 1300°C, the Knoop flaw grew by a factor of 10 before catastrophic failure. They also noted a decrease in slow crack growth at high temperatures with increasing crosshead speed. The fastest crosshead speed in the Petrovic study was 0.5 cm/min. With the impact nose velocity of 2700 cm/min used in this study, the lack of slow crack growth in the NC-132 at high temperatures is a reasonable observation.

The flaws on the Z-HPSN were identified and measured as shown in Table I. Twenty-two of the 25 Z-HPSN test bars fractured at the Knoop flaw. The other three test bars fractured from corner flaws which might have been caused by the surface finishing operations. None of the 13 test bars fractured at 1100°C or higher showed any sign of slow crack growth.

The Knoop flaws on the C-HPSN were difficult to identify and measure, as shown in Table II. This difficulty was caused by the coarser fracture surface of the C-HPSN; the flaws did not "stand out" under the microscope as they did on the other two materials. Many test bars of C-HPSN did not break at the Knoop flaw when tested above 1100°C. Of 12

test bars fractured at 1100°C or higher, eight broke at flaws other than Knoop flaws. In two cases the fracture flaws were clearly identified as oxidation pits. The possibility of slow crack growth in the C-HPSN could not be clearly evaluated. Although the two specimens tested at 1400°C had flaws 30% larger than room temperature specimens, this number is too small to draw a firm conclusion about slow crack growth.

C. Calculation of K_{IC}.

The Knoop hardness indenter introduces a semi-elliptical surface crack on the tensile side of the bend specimen. This surface flaw will grow catastrophically when the stress intensity at the flaw reaches a critical value. According to fracture mechanics theory, the stress intensity factor for a semi-elliptical surface flaw in bending is given by:[9,13]

$$K_{IC} = \sigma_f M (\pi a/Q)^{\frac{1}{2}} \quad (1)$$

where σ_f is the outer fiber tensile stress at fracture, M is a numerical factor related to flaw and beam geometry, a is the depth of the semi-elliptical flaw, and Q is given by:[9,13]

$$Q = \Phi - .212 (\sigma_f/\sigma_{ys})^2 \quad (2)$$

where σ^{ys} is the tensile yield stress of the material and $.212 (\sigma_f/\sigma_{ys})$ is a plastic zone correction factor. The value of σ_{ys} is so much larger than σ_f that this plastic zone correction factor is disregarded.[14] The term Φ is the elliptical integral:[13]

$$\Phi = \int_0^{\pi/2} (1 - \frac{c^2 - a^2}{c^2} \sin^2\theta)^{\frac{1}{2}} d\theta \quad (3)$$

which is tabulated in standard mathematical tables. The term c is the major axis of the semi-eliptical flaw.

The value for M was taken as 1.03, based upon bend tests by Petrovic et al.[9] on silicon nitride. Hung[15] used a value of 1.01 for test bars of silicon carbide of identical geometry to the test bars in this study. The difference in the two values of M does not introduce an error greater than that expected experimentally.

D. Room Temperature Strength & K_{IC}.

1. NC-132.

The NC-132 was tested at room temperature in three conditions -- no Knoop flaw, a 1000-g Knoop flaw, and a 2500-g Knoop flaw. The test data are given in Table II. As expected, the specimens with no Knoop flaw had the highest strength -- 990 MN/m^2 with a 12% variation among the four tests. This strength is higher than the strengths reported for NC-132 by other sources -- 867 MN/m^2 with 12% variation from the same billet by the manufacturer, 827 MN/m^2 with 12% variation by Larsen and Walther[1], and 614 MN/m^2 with 14% variation by Petrovic et al.[9] However, each of these tests had different surface finish parameters: Norton -- 8 RMS with a 320 grit diamond wheel, Larsen and Walther -- 12 RMS, and Petrovic -- 20 RMS. These differences in surface finish would account for the variation between observed bend strengths.

The surface finish was examined with the scanning electron microscope (SEM). The surface showed very few longitudinal scratches. The majority of flaws were pits formed by grain pullout and spalling. These pits were 1-10 microns in width and depth. They were similar to the flaw types observed on HPSN by Kossowsky[16], Kiehle et al.[17], and Rice[18].

The room temperature fracture surface showed both equiaxed and prismatic grains in the 1-5 micron size range. Fracture was a mixture of $\approx 30\%$ transgranular and $\approx 70\%$ intergranular.

The strength with the 1000-g and 2500-g flaws was less than the unflawed strength, as would be expected. The strength of the 2500-g flawed specimens (365 MN/m^2) compared well with the bend strengths for NC-132 test bars with 2600-g flaws (329 MN/m^2), tested by Petrovic et al.[9]

The K_{IC} values at room temperature are also given in Table II. The results obtained with a 2500-g flaw, 3.76 $MN/m^{3/2}$, compare well with Petrovic's[9] value of 3.6 $MN/m^{3/2}$.

2. Z-HPSN.

The Z-HPSN was not tested in the unflawed condition because of a shortage of material. The room temperature tests (Table III) gave bend strengths and K_{IC} values very close to those of the NC-132. Tests done by the fabricator showed bend strengths of 620 MN/m^2 at room temperature with an unspecified surface finish.

The surface flaws were again similar in size and shape to the "grain pull-out" flaws of the NC-132. The fracture surface showed a mixture of prismatic and equiaxed grains ranging in size between 1 and 10 microns. Fracture was more transgranular (50%) than observed on the NC-132.

3. C-HPSN.

The C-HPSN was tested in both the unflawed and Knoop-flawed condition (Table IV). The unflawed specimens had an average strength of 757 MN/m^2. Larsen and Walther[19] have tested material from the same source and found a room temperature 4-point bend strength of 530 MN/m^2 --

30% lower than that observed in this study. They mention the possibility of large isolated inclusions/pores or larger grain size as possible causes for the lower observed strengths as compared to NC-132.

The effect of surface finish must also be considered. The C-HPSN was polished with the 600-mesh SiC in the same manner as the NC-132. An SEM study of the surface showed fan-shaped regions of spalling 40 to 50 microns in width and length (Figure 3). These spalled regions were in marked contrast to the uniformly scattered 5-micron pits on the NC-132 surface. This difference is a possible explanation for the difference in strength for unflawed specimens between the two types of material.

In contrast to test results on the unflawed specimens, the strength of Knoop-flawed C-HPSN was 25% higher than the strength of Knoop-flawed NC-132. Differences in Knoop flaw dimensions were too small to account for the difference in fracture stresses. However, a study of the C-HPSN fracture surface showed a much more fibrous texture with a majority of thin prismatic grains 1-10 microns in length. Fracture was primarily intergranular with very little transgranular fracture. The prismatic grains looked as if many had been pulled out of the matrix.

Lange[20,21] had previously observed that hot-pressed silicon nitride had a "strong" and a "weak" direction. He related this difference to the mixture of equiaxed and prismatic grains. A greater percentage of prismatic grains gave a "fibrous" fracture surface and an increase in strength. Himsolt et al.[22] confirmed this observation and added that extended sintering times caused increased prismatic grain size and a lower bend strength.

These grain morphology and size effects are a possible explanation for the higher strength and K_{IC} at room temperature for the C-HPSN versus

the NC-132. The possibility of greater grain boundary strength must also be considered, as mentioned by Himsolt.[22] The observed strength of HPSN may be dependent in part on the intrinsic strength of the phase at the grain boundaries and how that phase bonds to the silicon nitride grains. Ceria-doping of silicon nitride may provide a stronger intergranular phase than that produced by magnesia-doping.

Petrovic et al.[9,23] observed that the room temperature of K_{IC} values obtained for HPSN with a Knoop flaw were lower than those observed in double torsion tests by Evans and Wiederhorn.[6] Petrovic annealed the Knoop-flawed specimens in air and in a low oxygen potential atmosphere at 1200°C and 1400°C. In subsequent fracture at room temperature the annealed specimens had much higher K_{IC} values. Petrovic et al. theorized that a residual stress relief mechanism and an oxidation flaw healing process were the source of the increase in strength and K_{IC}. A similar annealing study was done on the three varieties of hot-pressed silicon nitride in this study.

E. Annealing Effects on Room Temperature Strength and K_{IC}.

A study of annealing effects on the room temperature strength and K_{IC} of NC-132, C-HPSN, and Z-HPSN was done. The NC-132 and Z-HPSN were annealed at 1100°C in air and also in a nitrogen-0.1% hydrogen atmosphere. The C-HPSN was test annealed in both atmospheres and also across a range of temperatures -- 700°, 900°, and 1100°C. This was done because the prior high temperature fracture tests of the C-HPSN showed greater oxidation than the other materials. It was felt that this heavy oxidation layer on the C-HPSN would have a strong effect on the surface at lower temperatures.

The NC-132 was annealed in the conditions tabulated in Table II. The bend strengths and K_{IC} values are also given in that table. The increases in strength and K_{IC} match the annealing effects observed by Petrovic et al.[9] in slow bend tests and by Mendiratta et al.[7] in drop-weight impact tests. The increase in K_{IC} to the 5.25 $MN/m^{3/2}$ range compares well with the room temperature K_{IC} values determined in double torsion by Evans and Wiederhorn for HS-130 (4.7 $MN/m^{3/2}$) and also by Larsen and Walther[1] for NC-132 (5.25 $MN/m^{3/2}$).

The K_{IC} value obtained for the NC-132 annealed in the N_2/H_2 mixture is slightly less than that obtained by annealing in air. However, a comparison of the tensile surfaces of the differently annealed specimens showed that the surface of the N_2/H_2 annealed specimen had an oxide layer. That oxide layer was similar in appearance to the oxide layer of the air-annealed specimen. Both surfaces showed a base layer with white, prismatic crystals growing on the base layer. The N_2/H_2 oxidation layer was thinner and contained fewer and smaller prismatic crystals. A calculation of the oxygen activity in the N_2/H_2 mixture (based on H_2/H_2O equilibrium) gave an oxygen partial pressure of 10^{-15} atmospheres at 1100°C. The surface had oxidized even at this low oxygen partial pressure.

The K_{IC} values were equivalent for both the air and the N_2/H_2 annealing conditions. The mechanism of strength improvement over the unannealed flawed specimen cannot be clearly assigned to either the residual stress relief process or the oxidation healing process. Petrovic et al.[23] found evidence for both mechanisms. Work by Ziegler[24] on the healing of Knoop flaws in magnesia-doped hot-pressed Si_3N_4 showed a marked increase in strength after a 1-hour anneal at 1200°C. He postulated that the Knoop crack is healed by the formation of cristobalite and magnesium silicates on the surface above 900°C and by

viscous flow of the glass phase at higher annealing temperatures.

The Z-HPSN was annealed in the conditions tabulated in Table III. The strength and K_{IC} values increased by 60% for specimens annealed in air and by 28% for the specimens annealed in the N_2/H_2 mixture. This difference in strength improvement contrasts with the equal strength improvement seen in NC-132 in the two different atmospheres.

A comparison of the oxidized surfaces of the two annealed specimens showed the same oxidation pattern as seen in the NC-132. The air-annealed and N_2/H_2 annealed surfaces have similar morphologies; however, the N_2/H_2 annealed surface is less extensively oxidized. The similarities in annealing conditions and oxidation morphology between the Z-HPSN and the NC-132 do not explain the differences in strengths. This may reflect back on different properties of the oxides formed on the two materials. The presence of zirconia-based compounds may heal cracks less effectively.

None of the annealed Z-HPSN specimens broke at corner flaws or oxidation pits. However, it was more difficult to identify and measure the flaws on the annealed specimens as compared to the unannealed specimens. This is circumstantial evidence of oxidation in the Knoop flaw.

The C-HPSN was annealed in the conditions tabulated in Table IV. Annealing in air at 700°, 900°, and 1000°C universally increased the strength by 50% but with a great deal of data scatter. There was no dependence on the temperature. Annealing in the N_2/H_2 mixture showed a slow increase in strength and K_{IC} at 700°C and 900°C with a rapid increase to the air-anneal values with an 1100°C anneal. This distinction (temperature dependence in the N_2/H_2 atmosphere and no temperature dependence in air) again raises the question of what mechanisms are predominant at a given temperature.

Lange and Davis[25] observed that compressive stresses were developed in the oxidation layers of CeO_2-doped HPSN at temperatures between 400°C and 900°C. These compressive stresses raised the apparent strength. However, at the higher temperatures and after longer exposures the oxidation layer spalled and degraded and the strength dropped off rapidly.

A study of the surfaces of the 700°C annealed specimens showed no sign of oxidation under the SEM. Yet the two specimens showed markedly different strengths -- 902 MN/m^2 for the air anneal and 546 MN/m^2 for the nitrogen anneal. The measured flaw size on both specimens was 60 microns by 170 microns. Whether this strength difference depends on compressive stresses, crack healing, crack blunting, or residual stress relief cannot be determined.

In comparing the surfaces of the two C-HPSN specimens annealed at 1100°C in air and N_2/H_2, similar oxidation layers were observed -- a smooth base layer with white "button" growths on the surface. Again the N_2/H_2 annealed surface had a less extensively oxidized surface but with similar morphology. On both surfaces the pitted, spalled character of the underlying as-ground surface could still be seen.

There was difficulty in identifying the Knoop flaws on the annealed specimens. This difficulty, the limited number of specimens broken, and the question of what strengthening mechanisms are active limits the validity of the K_{IC} values for the annealed specimens. They should be considered as indicators of trends rather than firm values.

None of the annealing work was done at high enough temperatures or long enough times for pitting or bubbles to form in the oxide surface, as observed in other oxidation studies.[26] The mechanisms which could effect

the strength and the flaws would be limited to residual stress relief, crack healing and blunting, and imposed compressive stresses from oxide layers. The different effects of annealing at various temperatures, times, and atmospheres upon each type of HPSN again shows that the densifying additive has profound effects on the oxide layer (amount, morphology, inherent strength, adhesion to the base material, and growth kinetics).

F. High Temperature Strength and K_{IC}.

All the HPSN materials tested at high temperatures (1100°, 1250°, 1325°, and 1400°C) showed similar patterns for the fracture strength and K_{IC} values for impact as the temperature was raised. At 1100° and 1250°C the values for each material were at the same level or slightly higher than the values observed in the room temperature tests of the annealed material. Between 1250°C and 1400°C the fracture strength and K_{IC} values for impact loading dropped by 10-20%. None of the materials showed indications of slow crack growth in any high temperature test.

The strength and K_{IC} high temperature data for NC-132 are given in Table II. Values for these parameters across the 1100°-1250°C range are constant and agree with the room temperature tests of the annealed specimens (Figures 4 and 5).

Tests on NC-132 by Larsen and Walther[1] in 4-point slow bend showed a drop in strength at 1200°C as compared to room temperature. This drop in strength under slow bend conditions at 1200°C is common for magnesia-doped HPSN. Across the 1250°C-1400°C range the impact strength of NC-132 in this study dropped (17% to 423 MN/m^2). The 4-point bend strength on polished (12 RMS) NC-132 at 1350°C is 360 MN/m^2, as reported by Larsen and Walther[1]. The fact that a specimen with a 60 micron deep flaw is 16% stronger under impact than a similar specimen with no Knoop flaw under slow bending shows how important the strain rate is in determining strength.

The drop in slow bend strength at high temperatures is generally attributed to slow crack growth by grain boundary sliding. Under impact loading there is insufficient time for the plastic deformation mechanism (grain boundary sliding) to operate. This view is supported by the fact that no signs of slow crack growth in the NC-132 were observed at high temperatures. The measured depth of the Knoop flaws was in the 60 micron range for all specimens.

This strain rate effect on strength has been observed by Lange and Iskoe[5]. They noted that in tests of HS-130 above 1300°C the fracture stress increased as the load rate increased. At 1300°C an increase in load rate from 10 MN/m^2-min. to 1000 MN/m^2-min increased the fracture stress from 280 MN/m^2 to 450 MN/m^2.

Mendiratta et al.[7] conducted drop-weight impact tests on HS-130 with Knoop flaws at 1300°C and at room temperature (after annealing). The drop-weight velocity was 13,000 cm/min. They observed equal strengths at room temperature and 1300°C (550 MN/m^2) with no signs of slow crack growth. That study did not test above 1300°C.

An obvious oxide layer formed on the tensile surface of all the M-HPSN specimens tested at high temperatures. It might be expected that the properties of that oxide layer might change with increasing temperatures and have different effects on the Knoop flaw. However, all the NC-132 test bars broke at the Knoop flaw and the standard deviation of the strength data was no larger (5% on average) than the standard deviation on the room temperature data. The oxide layer did not seem to have an increasing blunting effect at higher temperatures (considering that all specimens were broken within 45 minutes of placement in the furnace). The Knoop flaw remained the largest active flaw on the specimen surface at all temperatures.

An SEM study of the oxide formations on the tensile surface of specimens tested at various temperatures showed oxide formations similar to those observed by Kiehle et al.[17] in their controlled oxidation studies on Norton HS-130 HPSN at similar temperatures. Kiehle et al.[17] first observed the formation of an amorphous silica layer at temperatures above 750°C. At long holding times at that temperature or at higher temperatures (1000°C) the silica layer devitrified to cristobalite (SiO_2). Above 1000°C magnesium and calcium silicates formed as needle-like crystals. The growth of those crystals increased with higher temperatures and longer times. Above 1350°C the Mg-silicate (enstatite) was observed to grow as rapidly as the cristobalite. Similar observations were made by Singhal[27] in oxidation of silicon nitride from 1100° through 1400°C.

Studies were made of the fracture surfaces of the NC-132 specimens broken at high temperatures. In all cases an oxide layer formed on the fracture surfaces immediately after fracture, regardless of how quickly specimens were removed from the furnace. This oxidation obscured the fracture surface and prevented evaluation of the mode of fracture -- transgranular or intergranular.

The critical stress intensity of NC-132 under impact was 5.25 $MN/m^{3/2}$ at 1100°C and 1250°C. This is comparable to the room temperature K_{IC} of annealed specimens. It agrees well with the double torsion tests on NC-132 at room temperature by Larsen and Walther[1] (5.25 $MN/m^{3/2}$ with 18% variation).

Above 1250°C the impact K_{IC} for NC-132 drops 5% at 1325°C and 15% at 1400°C. This drop in K_{IC} reflects back to the drop in fracture stress at these temperatures and the consistent flaw depth (60 microns).

Mendiratta et al.[7] observed a K_{IC} observed a K_{IC} of 5.5 $MN/m^{3/2}$ for impact tests of HS-130 at 1300°C, just slightly higher than the room temperature K_{IC} for their annealed specimens. This is in marked contrast to slow-bend tests in which K_{IC} increases dramatically with higher temperatures[1,9] as the grain boundary sliding process begins to operate. That process is an energy-absorbing mechanism which would be included among all the energy sinks considered in the effective fracture surface energy -- γ_i, where γ_i is related to K_{IC} by

$$K_{IC} = (2\gamma_i \, E/(1-\nu^2))^{\frac{1}{2}} \qquad (4)$$

where E is the elastic modulus and ν is Poisson's ratio.

Since the plastic deformation/grain boundary sliding process doesn't have sufficient time to occur, the effective fracture surface energy is not increased by the plastic work associated with grain boundary sliding. Any reasonable change in Poisson's ratio would be too small to cause a significant decrease in K_{IC}. Either the elastic modulus must decrease or the fracture surface energy must decrease to cause a decrease in K_{IC}.

If the observed decrease in impact K_{IC} at the 1400°C temperature is strictly a function of a decrease in elastic modulus, then the 15% K_{IC} decrease would be caused by a 27% decrease in elastic modulus. This calculated decrease in elastic modulus at 1400°C is less than the 43% decrease in secant modulus observed in 1350°C slow bending of NC-132 by Larsen and Walther[1].

The decrease in secant modulus at high temperatures, however, is a function of the viscoelastic grain boundary. Larsen and Walther also

tested reaction-bonded silicon nitride (RBSN) under identical conditions and observed a much smaller decrease in secant modulus (5% from room temperature to 1500°C). The RBSN does not have the grain boundary phase as a bonding agent between the silicon nitride grains.

In addition to changes in elastic modulus, a drecrease in the effective fracture surface energy is also possible. A decrease in the surface energy of the grain boundary material, less crack branching, or a change in the mode of fracture would all decrease the effective fracture surface energy. Such changes might manifest themselves as changes in the fracture surface. However, the oxidation of the fracture surfaces above 1250°C prevented any analysis.

Strength and K_{IC} data for the Z-HPSN are given in Table III and Figures 4 and 5. The Z-HPSN had higher strengths than the NC-132 at all temperatures. Those strengths had standard deviations not much larger than those observed for the NC-132 strengths. The Z-HPSN test bars also tended to break consistently at the Knoop flaw.

An SEM study of the oxide layer on the tensile surface of the Z-HPSN showed a similar silica-like base layer, as seen on the NC-132. On that base layer white "buttons" of material formed at 1100°C and were larger with higher test temperatures. No needle-like crystals were seen on the Z-HPSN at any temperature.

Hampton and Graham[29] did oxidation studies of zirconia-doped silicon nitride at 1400°C. Their studies showed two components in the oxide layer: cristobalite and a Si-Zr-O compound containing matrix impurities. They did not describe the morphology of the oxide layer.

The fracture surface of the Z-HPSN tested at 1100°C did not oxidize as extensively as the NC-132. The mode of fracture at 1100°C

was a mixture of transgranular and intergranular fracture. Fracture surfaces at higher test temperatures were again too heavily oxidized to study.

The critical stress intensity of the Z-HPSN dropped 35% across the 1250°-1400°C range. This change was larger than that observed in the NC-132. However, the Z-HPSN K_{IC} value at 1400°C (5.9 $MN/m^{3/2}$) was still 30% higher than the NC-132 K_{IC} value (4.46 $MN/m^{3/2}$) at the same temperature.

The Z-HPSN showed firm indications in this study of being a stronger material in impact than the NC-132. This contrasts with work by Larsen and Walther[19] in which Z-HPSN obtained from the same source was weaker in 4-point bend than NC-132 at both room temperature and 1500°C. This difference may depend on different responses to impact versus slow loading for the two materials. A more likely explanation would be differences between the two Z-HPSN billets. It was not determined if the Z-HPSN billet in this study and that of Larsen and Walther's study were identically fabricated.

Based on the results of this study it is hypothesized that the same mechanisms of fracture operate in both the Z-HPSN and NC-132. The temperature dependence of the strengths for the two materials are similar and differ only in magnitude. The differences in magnitude may depend on the different chemical character of the two grain boundary phases. A second possibility is a dependence on grain size, although the SEM study of the room temperature fracture surfaces showed larger grains in the Z-HPSN.

Strength and K_{IC} high temperature data for the C-HPSN are given in Table IV and Figures 4 and 5. These values show the same pattern as the temperature increases as observed in the NC-132 and the Z-HPSN.

An important difference between the C-HPSN and the other materials was that many of the C-HPSN specimens fractured did not break at the Knoop flaws. This was apparent from studies of the fracture surfaces and the much larger standard deviations in strength and K_{IC} values for the C-HPSN. Thus it cannot be assumed that the C-HPSN is stronger than NC-132 at higher temperatures. The valid comparison is that when identical flaws are introduced on NC-132 and C-HPSN, the C-HPSN has 30% higher strengths at 1100°C and 1250°C. It is theorized that the oxide layer forming on the C-HPSN changes the flaw character and affects the apparent strength. At 1400°C the NC-132 and C-HPSN have equivalent strengths; the drop in strength for the C-HPSN across the 1250°C-1400°C range is more severe than the same drop in NC-132.

High temperature slow-bend tests on Ceria-HPSN by Larsen and Walther[19] showed a similar strength-temperature dependence to that seen in NC-132, namely, a large decrease in strength above 1250°C. At 1500°C the strengths of the NC-132 and the Ceria-HPSN were equivalent in slow bend--180 MN/m^2.

The oxidation on the tensile surfaces of the C-HPSN were very similar in morphology to the oxidation on the NC-132. The only difference was that small white "buttons" of oxide were observed on the 1250°C surface of the C-HPSN, rather than the needle-like crystals. At 1400°C the C-HPSN oxidation did show the needle-like crystals. Lange[30] observed that all the cerium compounds in the Si_3N_4-SiO_2-Ce_2O_3 system oxidize at relatively low temperatures to CeO_2 and SiO_2. The same observation was made by Mah, Mazdiyasni, and Ruh[31].

The variability of the fracture flaws puts severe restrictions on the evaluation of K_{IC} for the C-HPSN. The number of flaws from which

K_{IC} could be calculated was limited. The identification and measurement of the flaw dimensions was much more difficult than on the NC-132. The K_{IC} values determined for the C-HPSN are higher than the comparable NC-132 values, but this may be dependent on major differences in flaw character (size, healing, blunting) rather than inherent differences in strength or K_{IC}.

The drop in K_{IC} for C-HPSN at 1400°C follows the same trend observed in NC-132. This may reflect again on temperature changes in the character of the grain boundary phase. As with the NC-132, excessive oxidation of the C-HPSN fracture surfaces at high temperatures prevented analysis of the mode of fracture.

Overall, the factors controlling the fracture strength and the K_{IC} for all these materials are the same for impact and for slow bend -- the size and condition of the critical flaw and the temperature dependent strength characteristics of the grain boundary phase. These materials are two-phase materials and this factor is critical in both theoretical analysis and experimental results. Up to 1250°C,oxidation on the tensile surface affects the surface flaws by healing or blunting or compressive stresses. The effect of that oxide must be considered in terms of the inherent strength, the molar volume changes, the way the oxide bonds to the surface, and the elastic modulus of the oxide. All these characteristics are strongly dependent on the oxide chemistry of the densifying agent and residual impurities, the oxidation temperature, and the exposure time.

Above 1250°C, the character of the grain boundary phase becomes critical, because at these higher temperatures the viscosity, the cohesive strength, and the fracture mechanisms in the grain boundary

phase change. All these properties are dependent again on the densifying agent and residual impurities.

Each different additive-silicon nitride system must be considered in this framework. The strength below 1250°C will depend on the effect of oxidation on the surface flaws. Above 1250°C additives which form more refractory compositions at grain boundaries or eliminate grain boundary phases entirely will exhibit better high temperature strength.

IV. CONCLUSIONS

Room temperature impact tests of the four materials with the 2500-g flaw indicate that the ceria-HPSN is the strongest material in impact, followed by the zirconia-HPSN and by the NC-132.

Annealing in atmospheres of varying oxygen potential and at various temperatures raised the room temperature impact strength and K_{IC} of all the materials. Although residual stress relief mechanisms may play a role in this strengthening, oxidation effects seem more critical. Each material oxidized differently in terms of morphology and severity. The oxide layers had varying effects on Knoop flaws -- the oxide on the C-HPSN "healing" the flaw and the oxides on the NC-132 and the Z-HPSN blunting the flaw.

At testing temperatures of 1100°C and 1250°C each material was as strong and had similar K_{IC} values in impact as observed for the annealed room temperature test specimens. No slow crack growth was observed on any specimen tested at these temperatures.

Above 1250°C the NC-132, the C-HPSN, and the Z-HPSN all showed decreases in impact strength and impact K_{IC} of 15% to 30% at the 1400°C level. The Knoop flaws in these high temperature tests again showed no

pattern of slow crack growth; this drop in strength and K_{IC} under impact is hypothesized to depend on the change in cohesive strength and/or fracture mechanisms of the intergranular phases at these higher temperatures.

Acknowledgements:

The research upon which this work is based was supported by AFOSR Grant No. 76-2920B. The measurements were carried out in the Ceramics Facility and Metallurgy Facility of Northwestern University's Materials Research Center, supported in part under the NSF-MRL program (Grant No. DMR76-80847).

References:

[1]D. C. Larsen and G. C. Walther, "Property Screening and Evaluation of Ceramic Vane Materials", Report #IITRI-D6114-ITR-24, Illinois Institute of Technology Research Institute, Chicago, IL, Oct. 1977.

[2]D. Richerson, "Effect of Impurities on the High Temperature Properties of Hot-Pressed Silicon Nitride", Am. Ceram. Soc. Bul., 52 [7] 560-562,569 (1973).

[3]E. M. Lenoe and G. D. Quinn, "Preliminary Creep Studies of Hot-Pressed Silicon Nitride", Deformation of Ceramics, Ed. R. Bradt, Plenum Press (1975), p. 399.

[4] D. C. Larsen, "Property Screening and Evaluation of Ceramic Vane Materials", Report IITRI-D6114-ITR-18, Illinois Institute of Technology Research Institute, Chicago, IL., Feb. 1977.

[5]F. F. Lange and J. L. Iskoe, "High Temperature Strength Behavior of Hot-Pressed Si_3N_4 and SiC: Effect of Impurities", Ceramics for High Performance Applications, Ed. Burke, Gorum, and Katz, Brook Hill Publ., (1974) p. 223.

[6]A. G. Evans and S. M. Wiederhorn, "Crack Propagation and Failure Prediction in Silicon Nitride at Elevated Temperatures", J. Mat. Sci., 9, 270 (1974).

[7]M. G. Mendiratta, J. Wimmer, and I. Bransky, "Dynamic K_{IC} and Dynamic Flexural Strength of HS-130 Si_3N_4", J. Mat. Sci. 12, 212 (1977).

[8]J. M. Wimmer and I. Bransky, "Impact Resistance of Structural Ceramics", Am. Ceram. Soc. Bul. 56 [6] 552-555,558 (1977).

[9]J. J. Petrovic, L. A. Jacobson, P. K. Talty, and A. K. Vasudevan, "Controlled Surface Flaws in Hot-Pressed Si_3N_4", J. Am. Ceram. Soc., 58 [3-4] 113-116 (1975).

[10]J. J. Petrovic and L. A. Jacobson, "Controlled Surface Flaws in Hot-Pressed SiC", J. Am. Ceram. Soc. 59 [1-2] 34 (1976).

[11]R. W. Rice and W. J. McDonough, "Hot-Pressed Si_3N_4 with Zr-based Additives", J. Am. Ceram. Soc. 58 [5-6] 264 (1975).

[12]S. T. Gonczy and D. L. Johnson, "Impact Fracture of Ceramics at High Temperature", Fracture Mechanics of Ceramics Vol. 3, Eds. R. C. Bradt, D.P.H.Hasselman and F. F. Lange, Plenum Press, N.Y., (1978), pp. 495-506.

[13]G. R. Marrs and C. W. Smith, "A Study of Local Stresses Near Surface Flaws in Bending Fields", Stress Analysis and Growth of Cracks, ASTM Spec. Tech. Publ. #512, p. 23 (1972).

[14]M. G. Mendiratta and J. J. Petrovic, "Slow Crack Growth from Controlled Surface Flaws in Hot-Pressed Si_3N_4", J. Am. Ceram. Soc. 61 [5-6] 226 (1978).

[15]D. T. Hung, "Instrumented High Temperature Impact Test of SiC", Masters Research Report, Northwestern University, Dept. of Materials Science and Engineering, 1978.

[16]R. Kossowsky, "Defect Detection in Hot-Pressed Si_3N_4", Ceramics for High Performance Applications, Ed. Burke, Gorum and Katz, Brook Hill Publ. (1974) p. 665.

[17]A. J. Kiehle, L. K. Herin, P. J. Gielisse, and T. J. Rockett, "Oxidation Behavior of Hot-Pressed Si_3N_4", J. Am. Ceram. Soc., 58 [1-2] 17 (1975).

[18]R. W. Rice, "Machining of Ceramics", Ceramics for High Performance Applications, Eds. Burke, Gorum and Katz, Brook Hill Publ. Co., (1974), p. 287.

[19]G. Walther, Illinois Institute of Technology Research Institute, Chicago, Il., Private Communication, April 1978.

[20]F. F. Lange, "Relation Between the Strength, Fracture Energy, and Microstructure of Hot-Pressed Si_3N_4", J. Am. Ceram. Soc. 56 [10] 518 (1973).

[21]F. F. Lange, "Fracture Toughness of Si_3N_4 as a Function of the Initial 2-Phase Content", J. Am. Ceram. Soc. 62 [7-8] 428 (1979).

[22]G. Himsolt, H. Knoch, H. Huebner, and F. W. Kleinlein, "Mechanical Properties of Hot-Pressed Silicon Nitride with Different Grain Structures", J. Am. Ceram. Soc. 62 [1-2] 29 (1979).

[23]J. J. Petrovic, R. A. Dirks, L. A. Jacobson, and M. G. Mendiratta, "Effects of Residual Stresses on Fracture from Controlled Surface Flaws", J. Am. Ceram. Soc. 59 [3-4] 177 (1976).

[24]G. Ziegler, "Crack Healing in Hot-Pressed Silicon Nitride", Ber. Dt. Keram. Ges., 55 [8] 397 (1978).

[25]F. F. Lange and B. I. Davis, "Development of Surface Stresses During the Oxidation of Several Si_3N_4/CeO_2 Materials", J. Am. Ceram. Soc., 62 [11-12] 629 (1979).

[26]S. M. Wiederhorn and N. J. Tighe, "Applications of Proof Testing to Silicon Nitride", Proc. Workshop Ceram. Adv. Heat Engines, 1977, pp. 247-58.

[27]S. C. Singhal, "Oxidation and Corrosion-Erosion Behavior of Si_3N_4 and SiC", Ceramics for High Performance Applications, Eds. Burke, Gorum and Katz, Brook Hill Publ. (1974) p. 533.

[28]A. G. Evans, R. W. Davidge, "The Strength and Oxidation Resistance of Reaction-Sintered Silicon Nitride", J. Mat. Sci., 5, 314 (1970).

[29]A. F. Hampton and H. C. Graham, "Oxidation of Hot-Pressed Si_3N_4 with Zr-Based Additives", Oxidation of Metals, 10 [4] 239 (1976).

[30]F. F. Lange, "High Temperature Mechanical Properties of Polyphase Ceramics Based on Silicon Nitride", Annual Report, Contract F49620-77-C-0072, Air Force Office of Scientific Research, March 1978.

[31]T. Mah, K. S. Masdiyasni, and R. Ruh, "The Role of Cerium Orthosilicate in the Densification of Si_3N_4", J. Am. Ceram. Soc., 62 [1-2] 12 (1979).

TABLE I

Measured Flaw Dimensions for 2500-g Flaw on Various HPSN

Sample/Test Conditions	Depth = a (microns)		Width - 2c (microns)		Number of Tests
	Av.	% S.D.	Av.	% S.D.	
NC-132					
Room Temperature					
No Anneal	66	2	157	3	4
Anneal - 1100°C					
Air - 2 hrs.	69	4	161	3	4
Air - 4 hrs.	69	14	163	2	4
N_2/H_2 - 2 hrs.	63	5	155	1	4
1100°C	65	11	164	12	8
1250°C	66	6	159	6	5
1325°C	70	8	160	8	8
1400°C	69	12	165	10	8
Z-HPSN					
Room Temperature					
No Anneal	60	8	157	4	3
Anneal - 1100°C					
Air - 2 hrs.	58	5	158	5	3
N_2/H_2 - 2 hrs.	58	5	157	5	3
1100°C	58	10	157	5	3
1250°C	52	7	155	5	2
1325°C	56	11	160	6	4
1400°C	66	14	167	5	4
C-HPSN					
Room Temperature					
No Anneal	66	7	173	5	4
All Air Anneal	60	12	171	10	5
All N_2/H_2 Anneal	59	13	163	6	6
1100°C	80	--	200	--	1
1250°C	70	--	165	--	1
1400°C	105	7	275	28	2

TABLE II

Bend Stress and K_{IC} for Impact Loading of NC-132

Test/Sample Condition	Bend Stress (MN/m^2)		K_{IC} ($MN/m^{3/2}$)		Number of Tests
	Aver.	% S.D.	Aver.	% S.D.	
Room Temp. No Anneal					
No Flaw	991	12	--	--	4
1000 g Flaw	471	4	4.17	2	2
2500 g Flaw	365	6	3.76	6	4
Room Temp. Annealed 1100°C					
2500 g Flaw					
Air - 2 hrs.	550	6	5.73	6	4
Air - 4 hrs.	530	5	5.48	3	4
N_2/H_2 - 2 hrs.	515	3	5.25	2	4
1100°C - 2500 g Flaw	503	7	5.15	6	8
1250°C					
1000 g Flaw	600	--	4.90	--	1
2000 g Flaw	570	7	5.37	8	5
2500 g Flaw	509	3	5.22	4	5
1325°C - 2500 g Flaw	482	4	4.98	3	8
1400°C - 2500 g Flaw	423	3	4.46	6	8

TABLE III

Bend Stress and K_{IC} for Impact Loading of Z-HPSN

Test/Sample Condition	Bend Stress (MN/m^2)			K_{IC} ($MN/m^{3/2}$)		Number of Tests
	Aver.	% S.D.	(#)	Aver.	% S.D.	
Room Temp. - 2500 g Flaw						
No Anneal	382	10		3.89	11	3
Anneal in Air 1100°C - 2 hrs.	629	16		6.41	18	3
Anneal in N_2/H_2 1100°C - 2 hrs.	488	14		4.96	11	3
1100°C - 2500 g Flaw	728	5	4	7.54	5	3
1250°C - 2500 g Flaw	774	2	4	7.92	5	2
1325°C - 2500 g Flaw	646	8		6.44	7	4
1400°C - 2500 g Flaw	561	5		5.90	2	4

TABLE IV

Bend Stress and K_{IC} for Impact Loading of C-HPSN

Test/Sample Condition	Bend Stress (MN/m^2)			K_{IC} ($MN/m^{3/2}$)		Number of Tests
	Aver.	% S.D.	(#)	Aver.	% S.D.	
Room Temp. No Anneal						
No Flaw	757	1		--	--	2
1500 g Flaw	569	5		5.03	3	2
2500 g Flaw	489	1		5.20	2	4
Room Temp. 2500 g Flaw						
Annealed 1 Hr. in Air						
700°C	800	18	2	10.2	--	1
900°C	861	1		8.89	1	2
1100°C	770	14		7.86	10	2
Annealed 1 Hr. in N_2/H_2						
700°C	532	4		5.60	6	2
900°C	556	10		5.58	5	2
1100°C	754	2		7.74	1	2
1100°C						
1500 g Flaw	723	-		7.97	--	1
2500 g Flaw	699	4	3	8.39	--	1
1250°C						
1500 g Flaw	593	-		6.47	--	1
2500 g Flaw	654	11		7.42	2	3
1400°C -- 2500 g Flaw	455	20		6.40	12	3

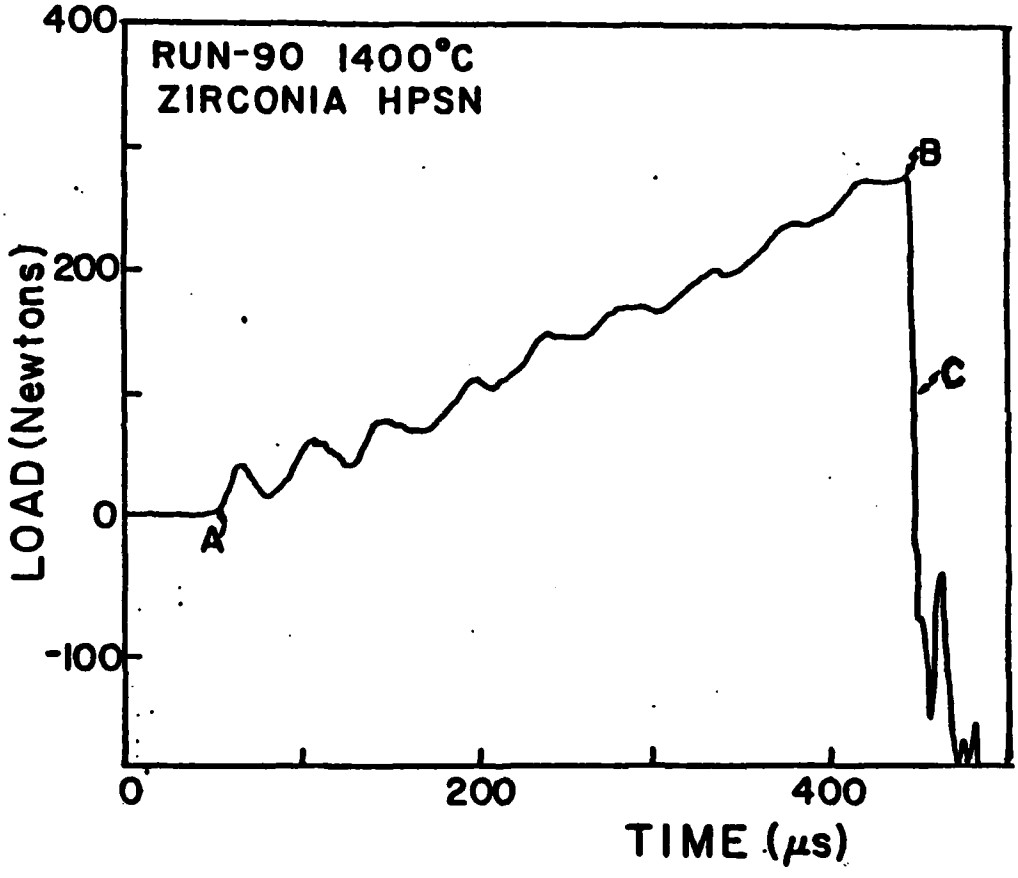

Figure 1: Typical Load-Time Trace

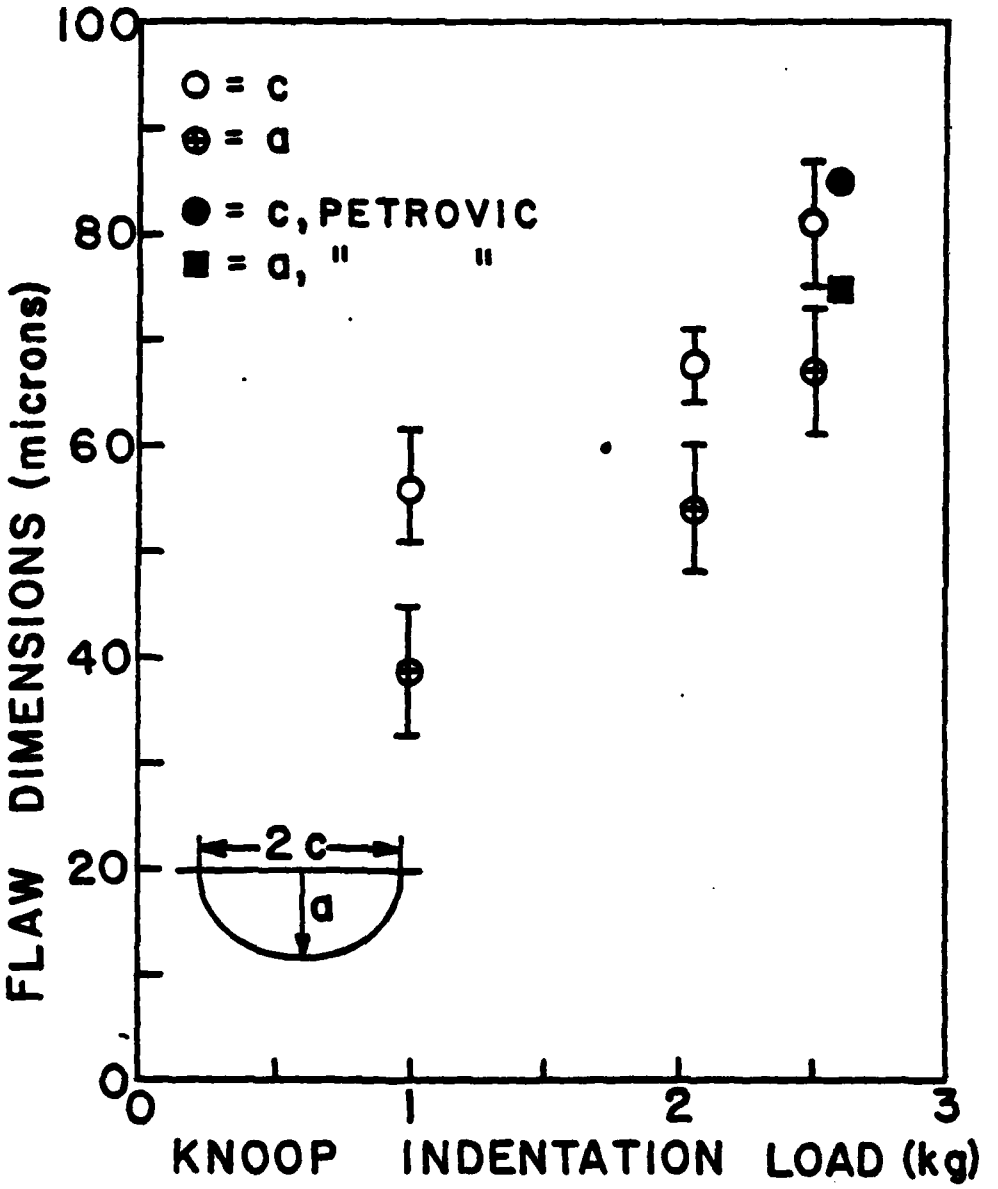

Figure 2: Knoop Flaw Dimensions for NC-132 Silicon Nitride as a Function of Load

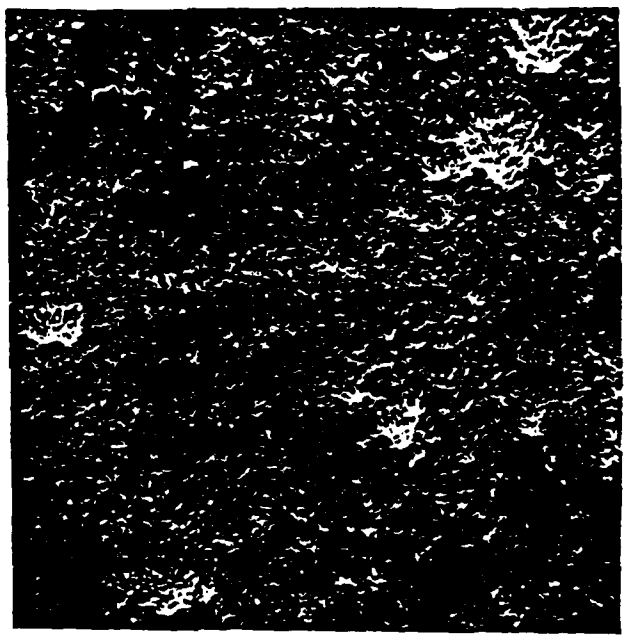

100 microns

Figure 3: Ceria-HPSN - #86 210X
Fractured at Room Temperature
Surface Finish after Final Grinding

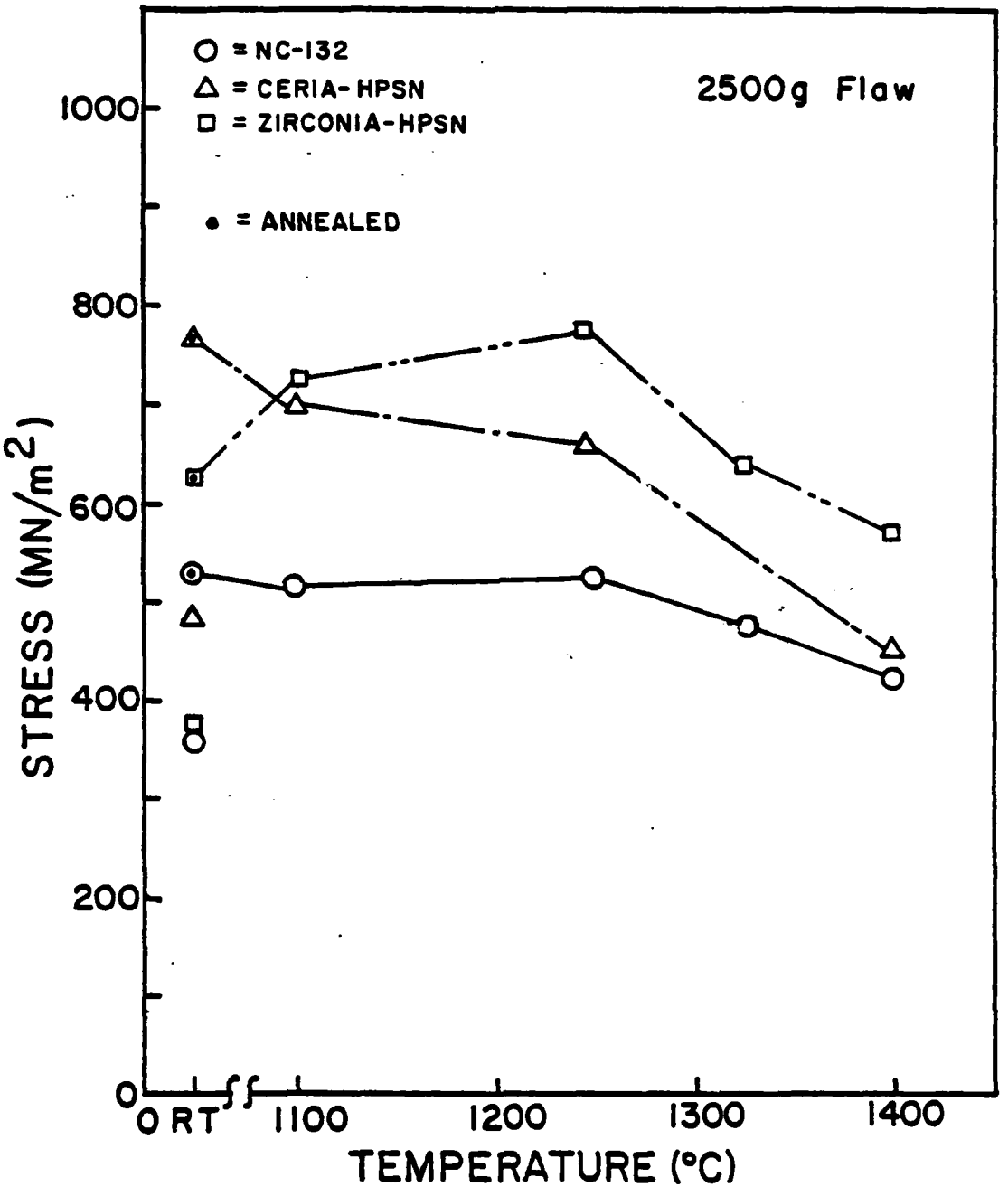

Figure 4: Impact Bend Strengths for All Tested Silicon Nitrides as a Function of Temperature

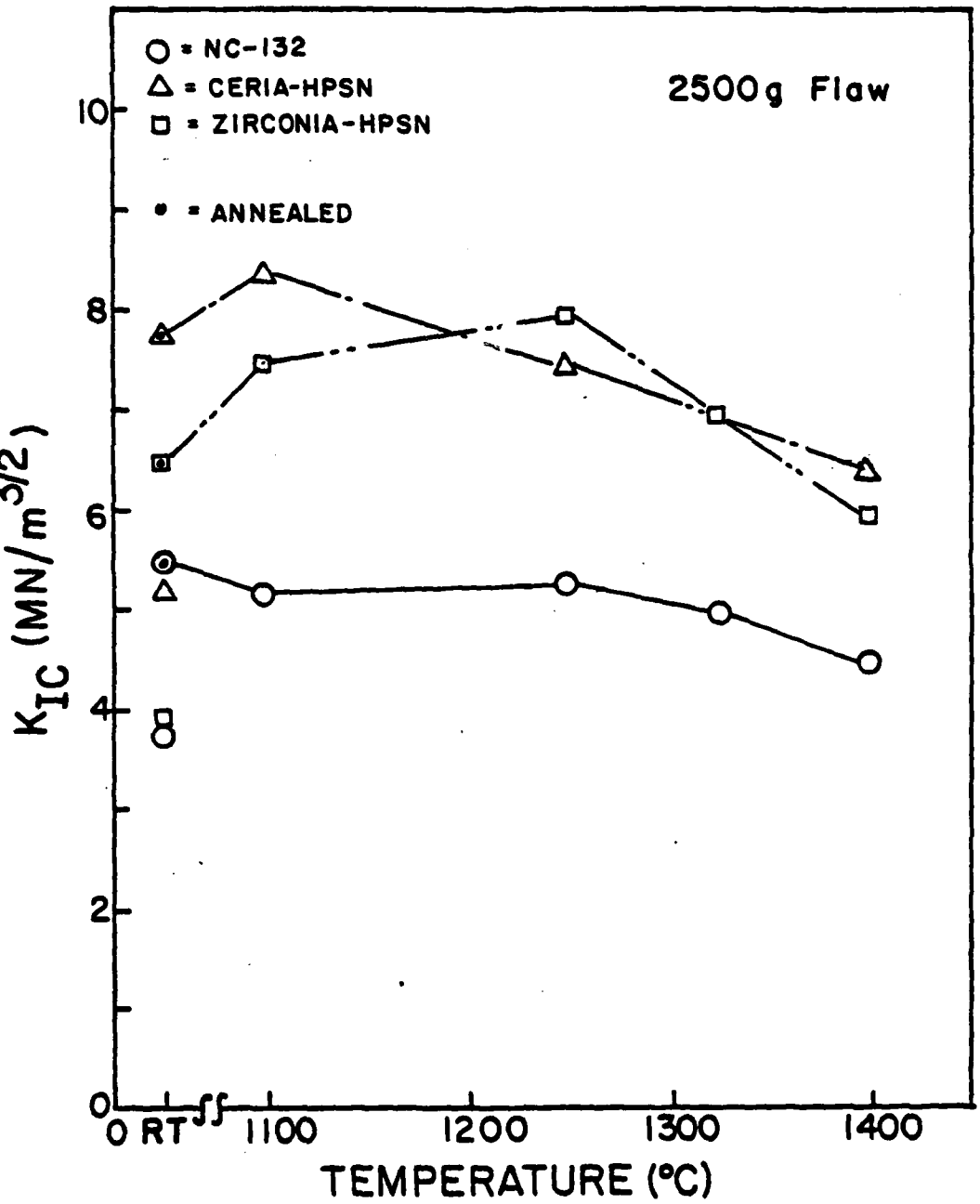

Figure 5: Impact Critical Stress Intensities for All Tested Silicon Nitrides as a Function of Temperature